Title
Manipulation of the unfolded protein response pathway by Legionella pneumophila

Author
Ibe, Nnejiuwa

Publication Date
2020

Peer reviewed|Thesis/dissertation

Manipulation of the unfolded protein response pathway by Legionella pneumophila

by
Nnejiuwa U. Ibe

DISSERTATION
Submitted in partial satisfaction of the requirements for degree of
DOCTOR OF PHILOSOPHY

in

Cell Biology

in the

GRADUATE DIVISION
of the
UNIVERSITY OF CALIFORNIA, SAN FRANCISCO

Approved:

DocuSigned by:
Shaeri Mukherjee
7AA908684B40471...

Shaeri Mukherjee
Chair

DocuSigned by:
Kaveh Ashrafi

Kaveh Ashrafi

DocuSigned by:
Anita Sil
9BCB4DFEE8384D2...

Anita Sil

Committee Members

Acknowledgements

My scientific development throughout graduate school has been influenced by many factors within and outside of the UCSF academic community. Family, friends, and mentors have supported me at every step and contributed towards my achievements thus far. Nothing I have done has been alone and without the help of others.

I must first thank the faculty and administrators of the UCSF Tetrad program. You saw something in my application that gave you faith that I would be a good candidate for the Tetrad program. I would not be the critical thinker I am now without the instruction from the various UCSF faculty members, courses, and discussion sessions designed to teach us how to think as scientists. I would also like to thank my classmates, all of whom provided inspiration and support over the years. Of note, I would like to thank Sumitra, Karina, and Efren for the support and encouragement at all stages in this process. The bonds we developed in our first year meant the world to me.

I extend the gratitude to the directors of many of the supplemental programs I have attended. This includes the IMSD staff, which provided me with a community in my early years at UCSF that helped build confidence in myself and my abilities. This also includes the staff of professional development programs like GSICE that provided me an opportunity to explore non-academic careers and build a professional network.

I am extremely grateful for my mentoring opportunities in the SEP program and SRTP program, where I was able to train undergraduate and high school students. I want to thank Thelma (Jay) Diaz-Santos, Haley Gause, and Tanya Kumar for being extremely

receptive learners. Each of you helped me further develop my mentoring skills and intensified my desire to pursue an academic career and train other students.

I am also grateful to those who mentored me throughout graduate school. I would like to thank the members of my thesis committee Dr. Kaveh Ashrafi and Dr. Anita Sil. Each of you helped steer my progress during the difficult transition in projects in my 3rd year. Your involvement in my success cannot be overstated and your scientific acumen has critically impacted my research progress. I have been extremely fortunate to have each of you as an intellectual resource and I value your support.

Science is not done in a silo, and as such I want to express my deepest gratitude to the people I have worked alongside throughout graduate school. This includes the members of the Hooper Foundation who provided a welcoming scientific community and research environment. This extends to the Hooper administrators and staff who made the science work in the background, and whose everyday contributions went generally un-noticed, but were instrumental towards my research progress.

More directly, I would like to thank past and present members of the Mukherjee lab. I have been fortunate to watch the lab develop as a scientific community and supportive environment where we could feel comfortable to share scientific ideas and random musings of the day. I would especially like to thank the early post-doctoral fellows in the lab, Elias Taylor-Cornejo and Philipp Schlaermann. Philipp was vital in the early progress on this project and developed many of the ideas and strategies utilized in my work. Elias has been a beacon of emotional stability in the lab and served as an example of professionalism. To the other postdoctoral fellows and graduate students in the lab, I am

extremely fortunate to have been able to work alongside you all. I expect the best out of each of you and I am confident you will succeed in your goals and endeavors.

Finally, and most importantly, I extend the most heartfelt thank you to my thesis advisor, PI, and mentor, Dr. Shaeri Mukherjee. Throughout my graduate experience, Shaeri has been the major contributor to my academic and personal growth. Her extraordinary intellect, persistent motivation, and genuine compassion helped push me through the most difficult goal I've pursued thus far. I've learned so much about science and life from Shaeri, and I am extremely grateful for her support in everything, especially the critical review of my manuscript and dissertation.

Manipulation of the unfolded protein response pathway by *Legionella pneumophila*

By

Nnejiuwa U. Ibe

Abstract

The intracellular bacterial pathogen *Legionella pneumophila (L.p.)* secretes over 300 bacterial proteins (effectors) to establish its replicative niche within host cells. Through its infectious life cycle, *L.p*. deploys its effectors to disrupt numerous host cell processes, including endoplasmic reticulum (ER) homeostasis. My dissertation explored the interaction between *L.p.* and the major homeostatic response pathway in the ER, the unfolded protein response (UPR). The results from my dissertation provide evidence that *L.p.* infection induces cleavage of the UPR sensor, activating transcription factor-6 (ATF6). Furthermore, I show that *L.p.*-mediated ATF6 cleavage is independent of proteasomal processing and does not require ER-associated degradation pathways. *L.p.* infection caused downstream activation of ATF6 target genes which include both lipid metabolism and proteostasis related genes. Interestingly, ATF6 activation during *L.p.* infection bypassed the requirement of conventional ATF6 pathway components. For example, chemical inhibition of ER to Golgi translocation of ATF6 with Ceapin A7 did not block its activation during *L.p*. infection. Furthermore, conventional site 1 and 2 protease (S1P and S2P) activities were dispensable during *L.p.* infection, as were the S1P and S2P cleavage sites on the ATF6 sensor. Additionally, time-lapse and confocal microscopy revealed that *L.p.*-mediated ATF6 activation bypasses ER to Golgi translocation and showed a direct recruitment of ATF6 to the *L.p.*-containing vacuole. Next, I compared ATF6 cleavage in the *L.p. Philadelphia* strain to the *L.p. Paris* strain, and showed that the *Paris* strain failed to

activate the ATF6 pathway. Bioinformatic comparison between the *Philadelphia* and *Paris strains* revealed 17 effectors that were unique to the *Philadelphia* strain. When individually expressed, *L.p*. effectors Lpg2131, Lpg0519, Lpg2523, and Lpg2465 could induce expression of an ATF6-specific luciferase reporter. Subsequent analysis showed that Lpg0519 could induce ATF6 processing without affecting other UPR sensors, such as PERK. Thus, my findings highlight the unique regulatory control that *L.p*. exerts upon the UPR sensors and discovers a novel strategy by which an intracellular bacterium can selectively perturb host homeostatic pathways.

Table of Contents

Chapter		Page
1-	**Introduction: Intracellular bacterial pathogens can serve as discovery tools of cell biology**	1
	References	11
2-	**Non-canonical activation of the ER stress sensor ATF6 by *Legionella pneumophila* effectors**	20
	References	55
3-	**Redundant targeting of the ATF6 pathway by *Legionella pneumophila* translocated substrates**	66
	References	80
4-	**Dissertation Conclusion**	82
	References	86

List of Figures

		Page
Figure 1.1	***L.p.* intracellular life cycle**	10
Figure 2.1	***L.p.* infection induces ATF6 processing independently of proteasomal degradation and ERAD.**	45
Figure 2.2	***L.p.* infection stimulates ATF6 target gene induction**	47
Figure 2.3	***L.p.* induces non-canonical activation of ATF6**	49
Figure 2.4	***L.p.* infection stimulates ATF6 nuclear recruitment**	51
Figure 2.5	***L.p. Paris* strain does not induce ATF6 processing**	53
Figure 3.1	**Lpg1960 induces ATF6 processing**	74
Figure 3.2	**GFP-Lpg1960 has a dimorphic localization pattern**	75
Figure 3.3	**Lpg1960 is not catalytically active against casein substrate**	76
Figure 3.4	**ATF6-like protein detected in *L.p.* lysates**	77
Figure 3.5	**Lpg2519 exhibits nuclear localization**	78
Figure 3.6	**Lpg2519 does not activate the ATF6 pathway**	79

List of Tables

Page

Table 3.1 **Bioinformatically identified *Legionella* effectors with protease homology** 73

Chapter 1

Introduction: Intracellular bacterial pathogens can serve as discovery tools of cell biology

Principles of Cell Biology

Even though higher order eukaryotes are made up of billions of cells that enable them to perform elaborate tasks, many organisms exist as single cells. Cells can be extremely diverse in their levels of organization and function. However, the fundamental principles that govern most life forms are remarkably conserved at the molecular level. Arguably, the most vital of these is the presence of genetic information that informs the cell on how to produce its building blocks and replicate itself.

The two major classes of cells include prokaryotes and eukaryotes. These two classes share many similar features including the presence and heritability of genetic material, proteins to perform structural and enzymatic function, and a selectively permeable barrier that controls what can enter and exit the cell. However, the differences between these two classes are what allow the complex molecular specialization within the cells. The most striking differences between the two classes are the compartmentalization of the genetic material and the compartmentalization of biochemical activities and cellular processes within the cell [2]. Prokaryotes have no nucleus to enclose the genetic information, whereas eukaryotes compartmentalize their genetic material within a nucleus. Secondly, all biochemical activities of a prokaryote exist on or within the single compartment that is the cell. However, eukaryotes contain membrane-bound organelles which are unique subcellular compartments with distinctive structural, macromolecular, and biochemical features.

Organelles within eukaryotic cells permit the sequestration of components needed to perform specialized tasks within the cell [3, 4]. The isolated environments serve to benefit cellular fitness because they enable coordination and regulation of specific metabolic tasks to increase efficiency and control without interference from other cellular processes [4]. In fact, the proteome, lipid composition, and enclosed environment of an organelle will often be substantially different than the rest of the cell [5]. For example, the specialized lipid cardiolipin can be found in greatest abundance within the mitochondrial inner membrane, enabling specialized signaling responses to occur at the mitochondria [6].

Aside from the nucleus, one of the most vital subcellular compartments within a eukaryotic cell is the endoplasmic reticulum (ER). The ER is a vast interconnected membranous network that forms a labyrinth throughout the cell. The ER is a major site for lipid and protein biosynthesis, and the inter-organelle interaction between the ER and nearly all other organelles highlights its central role in a variety of cellular processes [7, 8]. A major physiological function of the ER is to serve as the entry point to the secretory pathway for nearly one-third of newly synthesized proteins [9]. The ER houses specialized machinery to help fold nascent proteins and covalently modify them with post-translational modifications [10, 11]. Additionally, the ER architecture is maintained by domain-specific scaffolding proteins that are important for the formation of the elaborate tubular structures and the stabilization of sheet structures [12]. As such, understanding the biological processes of various organelles is critical towards understanding molecular mechanisms within the cell.

The molecular mechanisms that govern biological processes present a blueprint for life. Understanding cellular functions and how various pathways in our cells work together to maintain homeostasis in an ever-changing environment are the underpinnings of cell biology. Shortly after the introduction of cell theory in the late 1900's, German physician/pathologist Rudolf Virchow postulated that the pathology of an organism is the result of cellular pathology which brought to pass the idea that pathological alterations to normal cellular function can cause disease [13]. Using this reductionist comparative approach, biologists have uncovered significant information about various cellular functions, and researchers have since continued to devise new strategies to compare normal cellular function to a perturbed state.

Studying Biological Processes During Cellular Perturbations

In modern biology, one of the most successful strategies in identifying cellular regulators is through pharmacological and genetic perturbations [14, 15]. Early developments in molecular genetics introduced mechanisms to induce mutations within the genome and characterize how these perturbations alter cellular functions [16, 17]. Progressive developments, including the use of yeast artificial chromosomes and recombinant DNA technology permitted the exogenous expression of transgenes and regulatory sequences that facilitated the advancement in our understanding of gene function in biology [18, 19]. The more recent advances in genetic tools, like the CRISPR/Cas9 system, in combination with data from large scale projects to map the entire genomes of various species, now allow researchers to further elucidate the functions of gene and protein networks [20, 21]. Though these advances in genetic analysis have

provided excellent tools for unbiased investigations of cellular processes, additional perturbation strategies exist that allow for more targeted investigations.

A very successful perturbation strategy involves the use of pathogenic microorganisms that subvert eukaryotic cell function. Pathogens have been shown to utilize a diverse range of strategies to overcome, undermine, reprogram, or co-opt various eukaryotic processes to promote survival [22]. Intracellular pathogens that replicate and survive within the host cell have adopted unique strategies to exploit and modify host cell processes. They participate in a very sophisticated arms race with their host. Even though they disrupt host cell function to ensure survival, this disruption is not severe enough for host cell death, thus allowing for pathogen replication [51]. This balance between toxicity and survival is the result of intricate strategies to target host cell components. Classical examples of cellular processes perturbed under pathogenic infection include targeted disruption of the cytoskeletal network, membrane trafficking pathways, and signal transduction pathways [23-25]. More so, it is very common for pathogens to use virulence factors to target vital regulatory proteins within the host cell and early on it was realized that studying how pathogens manipulate host responses not only allows us to understand more about pathogenic strategies, but also provides insight into fundamental biological principles. Thus, pathogenic microorganisms have become common tools for cell biologists.

Cell biologists have realized practical applications from the study on microbial pathogenesis. Several pathogens, including *Yersinia spp*., make use of cytoskeletal functions to induce internalization of the pathogen and increase invasiveness [28]. The *Yersinia pseudotuberculosis* virulence protein, invasin, was shown to interact with eukaryotic

integrin family proteins [29]. This interaction triggered cystokeletal rearrangements of actin, talin, and filamin to promote bacterial uptake [30]. Unlike *Yersinia spp.* that target cytoskeletal elements from outside the cell, *Listeria monocytogenes* and *Shigella flexneri* target actin and actin regulators intracellularly [53]. When studying *Listeria monocytogenes* infection, researchers observed the rearrangement of actin cytoskeletal elements that enabled the pathogen to spread intercellularly [26, 31]. Through these observations, it was shown that the bacterial surface protein, ActA, was important for the recruitment of actin polymerization factors [32]. The subsequent purification of actin polymerization-promoting factors led to the identification of the Arp2/3 complex as the factor to initiate actin polymerization at the bacterial surface [33]. Importantly, these discoveries contributed to our fundamental understanding of actin dynamics and cytoskeletal regulation [27].

Legionella pneumophila subverts host cell processes

The intracellular bacterial pathogen, *Legionella pneumophila (L.p.),* has also emerged as an excellent tool to study biological mechanisms. During infection, *L.p*. is internalized and uses a specialized Dot/Icm Type IV secretion system (T4SS) to translocate over 300 effector proteins into the eukaryotic host cytosol [38]. Beyond the sheer number of translocated effectors, these T4SS substrates use sophisticated strategies such as novel post-translational modifications, unique catalytic mechanisms, and molecular mimicry of eukaryotic proteins, to disrupt host cellular processes including membrane trafficking pathways [34-37, 42] [39-41].

Formation and maturation of the *Legionella*-containing vacuole (LCV), involves diversion away from the endocytic pathway and the establishment of an ER-like replicative niche [39, 44] [**Figure 1.1**]. Investigations into *L.p*. mediated subversion of membrane trafficking pathways revealed an intricate control over host GTPase proteins [43]. In fact, targeting of host Rab1 and Arf1 GTPases are vital to vacuolar maturation, yet they function independently and are targeted by *L.p*. effectors in distinct ways [44, 45]. *L.p*. effectors DrrA and AnkX dynamically regulate Rab1 function, in part, through post-translational modification of the switch II region with AMPylation and phosphocholination, respectively [46, 47]. These Rab1 modifications disrupt interactions between Rab1 and Rab1 regulators like the Rab1 GDP dissociation inhibitor (GDI) [48]. Similar to Rab1, the Arf1 GTPase is also targeted by *L.p*. effectors during infection. In the case of Arf1, the *L.p*. effector RalF uses an intrinsic GEF activity and induces recruitment of Arf1 to the LCV which in turn promotes the recruitment of ER-markers to the intravacuolar compartment [52]. These results also allowed researchers to speculate whether eukaryotic cells utilize similar mechanisms outside of an infection setting.

The interaction between the LCV and ER occurs very early during infection and takes on different forms throughout the intracellular life cycle and as vacuolar maturation progresses. In fact, the importance of the ER in *L.p*. infection precedes internalization, as perturbations in ER calcium stores were shown to negatively impact *L.p*. uptake into host cells [49]. However, once inside the cell, ER luminal markers, including calnexin, are detected on the LCV within 60 minutes [50]. The dynamic tubular network of the ER is maintained by several GTPase families as well as membrane-shaping proteins [55]. Multiple smooth ER proteins are recruited to the LCV at early stages of infection, including

the ER curvature-generating protein, Reticulon 4 (Rtn4). Targeting of Rtn4 during infection involves recruitment to the LCV and post-translational ubiquitination by the Sde family of effectors [54]. Interaction between Sde family members and Rtn4 was shown to induce structural rearrangements of ER tubules around the LCV. Additional proteins known to regulate tubular ER dynamics have also been shown to play important roles in LCV maturation. The ER tubule GTPase Atlastin3 (Atl3) was shown to be important for the recruitment of ER markers, and RNAi-mediated knockdown of Atl3 in RAW 264.7 macrophages reduced bacterial growth by nearly 50% [56]. Altogether, these ER-LCV associations are critical to the establishment of a replication-competent compartment within the host cell.

Disruption of ER homeostasis by pathogenic infection

The ER is the major entry point for the production and trafficking of many proteins and lipids within the cell, as well as a vital site for maintaining cellular calcium homeostasis [57-59]. The ER is sensitive to a variety of intrinsic and extrinsic perturbations that can affect ER function and lead to an accumulation of unfolded proteins or misfolded proteins [60]. Under these conditions, the ER triggers an adaptive response known as the unfolded protein response (UPR). The UPR is an inter-organelle signaling network mediated by three ER transmembrane sensors: PRK-like ER kinase (PERK), inositol-requiring transmembrane kinase/endonucleases (IRE1), and activating transcription factor 6 (ATF6) [61]. In each case, an ER stress signal is detected by the luminal domains to induce a cascade of events that together lead to alterations in mRNA stability, repression of global translation, and induction of stress-responsive transcriptional programs [62].

Though the UPR is primarily thought to safeguard protein-folding capacity within the ER, additional cellular signals integrate into the UPR pathway including Toll-like receptor (TLR) stimulation and pathogen infection [63]. During infection, microbial pathogens are detected by pathogen recognition receptors (PRR), such as TLRs [64]. Upon stimulation, it was shown that TLRs can engage the UPR by activation of the IRE1 pathway and induction of XBP1 splicing. It was also reported that PERK can directly and indirectly regulate the NF-κB pathway. The impact of UPR activation during pathogen infection was shown to promote the production of pro-inflammatory molecules and in many cases, UPR induction restricts pathogen replication [65, 66]. Yet non-PRR dependent activation of the UPR also occurs during infection. Of note, intracellular pathogens that interact with the ER can interfere with its homeostatic functions. The single-stranded RNA virus Hepatitis C virus (HCV) depends on the ER for processing of its viral envelope proteins, formation of viral replication complex, as well as egress of budding viral particles through the secretory pathway. HCV can elicit activation of all three arms of the UPR [67].

Some pathogens are capable of subverting or exploiting one or more UPR functions for the benefit of survival and replication within the host [68]. The chlamydial organism *Simkania negevensis* forms extensive interactions with the ER and triggers UPR induction. However, through the course of infection the ER-stress response is downregulated allowing for the formation of its vacuolar compartment and bacterial growth [69]. In contrast, the bacterial pathogen *Brucella abortus* can target the UPR through the use of the T4SS effector VceC, which was shown to localize to the ER and interact with the UPR master regulator, BiP/GRP78 [70]. In the case of *B. abortus*, UPR induction was shown to enhance bacterial replication [71].

As the intracellular life cycle of *L.p*. involves substantial interactions with the smooth and rough ER [72, 73], our lab investigated how this interaction might impact ER homeostasis and UPR activation during infection. To our surprise, *L.p*. was shown to differentially regulate various arms of the UPR [74]. Our laboratory identified five *L.p*. encoded glucosyltransferases (Lgt) that can inhibit the IRE1 arm of the UPR when individually expressed. It was shown that exogenous expression of the Lgt family of effectors could block IRE1 mediated splicing of XBP1 upon chemical induction of the UPR. Though the IRE1 pathway was inhibited during *L.p*. infection, the study also revealed activation of the ATF6 pathway. However, the mechanisms by which ATF6 is activated was not clear. In **Chapter 2**, I present the results of my thesis work that reveal a novel, non-canonical mode of ATF6 activation.

Figure 1.1

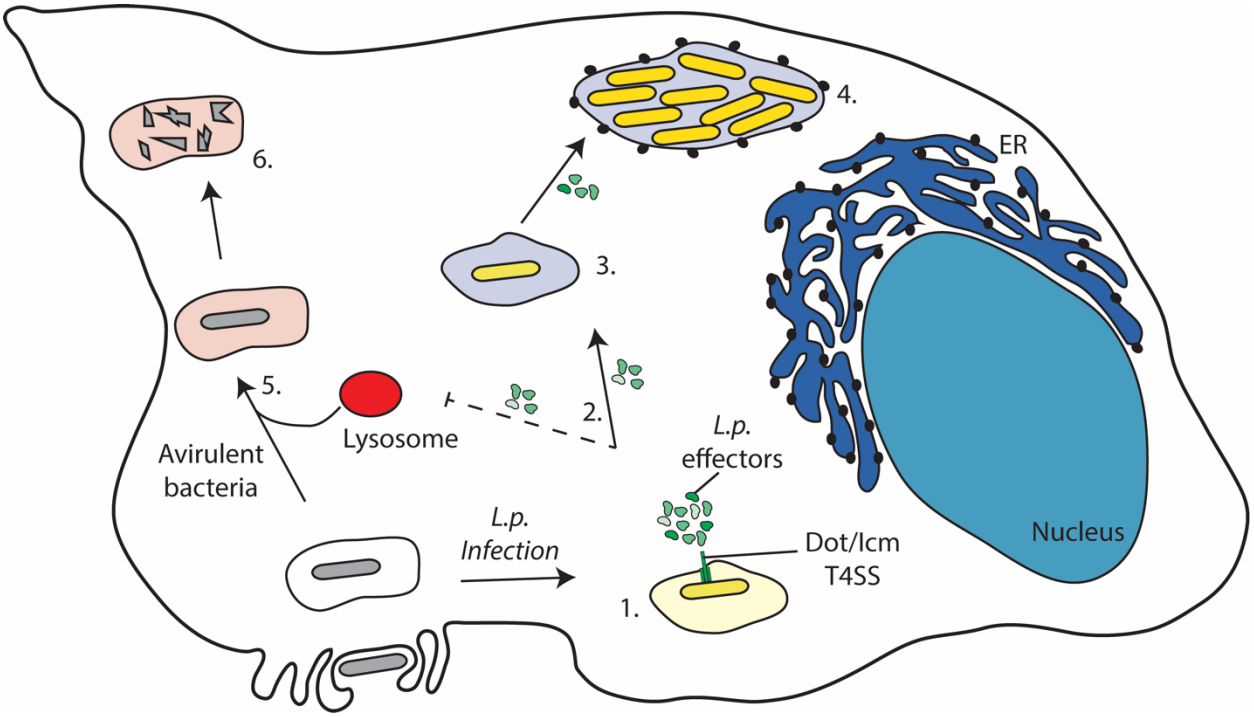

Figure 1.1: *L.p.* intracellular life cycle

Upon uptake, *L.p.* injects effector proteins (green) into the host cell through the Dot/Icm type IV secretion system (1). Secreted effectors allow *L.p.* to acquire early ER markers (blue) and escape the default endo-lysosomal pathway (2-3). The LCV is slowly transformed into a ribosome-studded compartment that mimics host-cell rough ER and supports replication of *L.p.* (4). Phagosomes containing an avirulent bacterium traffic along the endosomal route and eventually fuses with the lysosome (5), which kills and degrades the bacterium (6).

References

1) Alberts, B., Johnson, A., Lewis, J., Raff, M., Roberts, K., & Walter, P. (2002). The chemical components of a cell. In Molecular Biology of the Cell. 4th edition. Garland Science.
2) Alberts, B., Johnson, A., Lewis, J., Raff, M., Roberts, K., & Walter, P. (2002). The compartmentalization of cells. In Molecular Biology of the Cell. 4th edition. Garland Science.
3) Campbell, P. N., & Blobel, G. (1976). The role of organelles in the chemical modification of the primary translation products of secretory proteins. FEBS letters, 72(2), 215-226.
4) De Duve, C. (1963). The lysosome. Scientific American, 208(5), 64-73.
5) Heald, R., & Cohen-Fix, O. (2014). Morphology and function of membrane-bound organelles. Current opinion in cell biology, 26, 79-86.
6) Munro, S. (2004). Organelle identity and the organization of membrane traffic. Nature cell biology, 6(6), 469-472.
7) Dudek, J. (2017). Role of cardiolipin in mitochondrial signaling pathways. Frontiers in cell and developmental biology, 5, 90.
8) Kornmann, B., & Walter, P. (2010). ERMES-mediated ER-mitochondria contacts: molecular hubs for the regulation of mitochondrial biology. Journal of cell science, 123(9), 1389-1393.
9) Wu, H., Carvalho, P., & Voeltz, G. K. (2018). Here, there, and everywhere: The importance of ER membrane contact sites. Science, 361(6401).

10) Rothman, J. E., & Orci, L. (1992). Molecular dissection of the secretory pathway. Nature, 355(6359), 409-415.

11) Aebi, M. (2013). N-linked protein glycosylation in the ER. Biochimica et Biophysica Acta (BBA)-Molecular Cell Research, 1833(11), 2430-2437.

12) Westrate, L. M., Lee, J. E., Prinz, W. A., & Voeltz, G. K. (2015). Form follows function: the importance of endoplasmic reticulum shape. Annual review of biochemistry, 84, 791-811.

13) Schultz, M. (2008). Rudolf virchow. Emerging infectious diseases, 14(9), 1480.

14) Csermely, P., Korcsmáros, T., Kiss, H. J., London, G., & Nussinov, R. (2013). Structure and dynamics of molecular networks: a novel paradigm of drug discovery: a comprehensive review. Pharmacology & therapeutics, 138(3), 333-408.

15) Griffiths, A. J., Gelbart, W. M., Lewontin, R. C., & Miller, J. H. (2002). Modern genetic analysis: integrating genes and genomes (Vol. 1). Macmillan.

16) Bourre, F., & Sarasin, A. (1983). Targeted mutagenesis of SV40 DNA induced by UV light. Nature, 305(5929), 68-70.

17) Gentil, A., Margot, A., & Sarasin, A. (1986). 2-(N-acetoxy-N-acetylamino) fluorene mutagenesis in mammalian cells: sequence-specific hot spot. Proceedings of the National Academy of Sciences, 83(24), 9556-9560.

18) Lamb, B. T., & Gearhart, J. D. (1995). YAC transgenics and the study of genetics and human disease. Current opinion in genetics & development, 5(3), 342-348.

19) Micklos, D. A., Freyer, G. A., & Lauter, S. Z. (1990). DNA science: A first course in recombinant DNA technology (pp. 256-257). Carolina Biological Supply Company.

20) Doudna, J. A., & Charpentier, E. (2014). The new frontier of genome engineering with CRISPR-Cas9. Science, 346(6213).

21) Hsu, P. D., Lander, E. S., & Zhang, F. (2014). Development and applications of CRISPR-Cas9 for genome engineering. Cell, 157(6), 1262-1278.

22) Bhavsar, A. P., Guttman, J. A., & Finlay, B. B. (2007). Manipulation of host-cell pathways by bacterial pathogens. *Nature*, *449*(7164), 827-834.

23) Lemichez, E., & Aktories, K. (2013). Hijacking of Rho GTPases during bacterial infection. Experimental cell research, 319(15), 2329-2336.

24) Stegmann, T., Doms, R. W., & Helenius, A. (1989). Protein-mediated membrane fusion. Annual review of biophysics and biophysical chemistry, 18(1), 187-211.

25) Shames, S. R., Auweter, S. D., & Finlay, B. B. (2009). Co-evolution and exploitation of host cell signaling pathways by bacterial pathogens. The international journal of biochemistry & cell biology, 41(2), 380-389.

26) Cossart, P. (2000). Actin-based motility of pathogens: the Arp2/3 complex is a central player: Microreview. Cellular microbiology, 2(3), 195-205.

27) Pizarro-Cerdá, J., & Cossart, P. (2006). Subversion of cellular functions by Listeria monocytogenes. The Journal of Pathology: A Journal of the Pathological Society of Great Britain and Ireland, 208(2), 215-223.

28) Rosenshie, I., & Finlay, B. B. (1993). Exploitation of host signal transduction pathways and cytoskeletal functions by invasive bacteria. Bioessays, 15(1), 17-24.

29) Isberg, R. R., Voorhis, D. L., & Falkow, S. (1987). Identification of invasin: a protein that allows enteric bacteria to penetrate cultured mammalian cells. Cell, 50(5), 769-778.

30) Young, V. B., Falkow, S., & Schoolnik, G. K. (1992). The invasin protein of Yersinia enterocolitica: internalization of invasin-bearing bacteria by eukaryotic cells is associated with reorganization of the cytoskeleton. The Journal of cell biology, 116(1), 197-207.

31) Tilney, L. G., & Portnoy, D. A. (1989). Actin filaments and the growth, movement, and spread of the intracellular bacterial parasite, Listeria monocytogenes. The Journal of cell biology, 109(4), 1597-1608.

32) Kocks, C., Gouin, E., Tabouret, M., Berche, P., Ohayon, H., & Cossart, P. (1992). L. monocytogenes-induced actin assembly requires the actA gene product, a surface protein. Cell, 68(3), 521-531.

33) Welch, M. D., Iwamatsu, A., & Mitchison, T. J. (1997). Actin polymerization is induced by Arp 2/3 protein complex at the surface of Listeria monocytogenes. Nature, 385(6613), 265-269.

34) Qiu, J., & Luo, Z. Q. (2017). Hijacking of the host ubiquitin network by Legionella pneumophila. Frontiers in cellular and infection microbiology, 7, 487.

35) Ge, J., & Shao, F. (2011). Manipulation of host vesicular trafficking and innate immune defence by Legionella Dot/Icm effectors. Cellular microbiology, 13(12), 1870-1880.

36) Weber, S. S., Ragaz, C., Reus, K., Nyfeler, Y., & Hilbi, H. (2006). Legionella pneumophila exploits PI (4) P to anchor secreted effector proteins to the replicative vacuole. PLoS Pathog, 2(5), e46.

37) Sherwood, R. K., & Roy, C. R. (2016). Autophagy evasion and endoplasmic reticulum subversion: the yin and yang of Legionella intracellular infection. Annual review of microbiology, 70, 413-433.

38) Christie, P. J., & Vogel, J. P. (2000). Bacterial type IV secretion: conjugation systems adapted to deliver effector molecules to host cells. Trends in microbiology, 8(8), 354-360.

39) Lin, Y. H., & Machner, M. P. (2017). Exploitation of the host cell ubiquitin machinery by microbial effector proteins. Journal of cell science, 130(12), 1985-1996.

40) Allombert, J., Fuche, F., Michard, C., & Doublet, P. (2013). Molecular mimicry and original biochemical strategies for the biogenesis of a Legionella pneumophila replicative niche in phagocytic cells. Microbes and Infection, 15(14-15), 981-988.

41) Roy, C. R., & Mukherjee, S. (2009). Bacterial FIC proteins AMP up infection. Science signaling, 2(62), pe14-pe14.

42) Bärlocher, K., Welin, A., & Hilbi, H. (2017). Formation of the Legionella replicative compartment at the crossroads of retrograde trafficking. Frontiers in Cellular and Infection Microbiology, 7, 482.

43) Hardiman, C. A., McDonough, J. A., Newton, H. J., & Roy, C. R. (2012). The role of Rab GTPases in the transport of vacuoles containing Legionella pneumophila and Coxiella burnetii.

44) Kagan, J. C., & Roy, C. R. (2002). Legionella phagosomes intercept vesicular traffic from endoplasmic reticulum exit sites. Nature cell biology, 4(12), 945-954.

45) Arasaki, K., Toomre, D. K., & Roy, C. R. (2012). The Legionella pneumophila effector DrrA is sufficient to stimulate SNARE-dependent membrane fusion. Cell host & microbe, 11(1), 46-57.

46) Müller, M. P., Peters, H., Blümer, J., Blankenfeldt, W., Goody, R. S., & Itzen, A. (2010). The Legionella effector protein DrrA AMPylates the membrane traffic regulator Rab1b. Science, 329(5994), 946-949.

47) Tan, Y., Arnold, R. J., & Luo, Z. Q. (2011). Legionella pneumophila regulates the small GTPase Rab1 activity by reversible phosphorylcholination. Proceedings of the National Academy of Sciences, 108(52), 21212-21217.

48) Oesterlin, L. K., Goody, R. S., & Itzen, A. (2012). Posttranslational modifications of Rab proteins cause effective displacement of GDP dissociation inhibitor. Proceedings of the National Academy of Sciences, 109(15), 5621-5626.

49) Fajardo, M., Schleicher, M., Noegel, A., Bozzaro, S., Killinger, S., Heuner, K., ... & Steinert, M. (2004). Calnexin, calreticulin and cytoskeleton-associated proteins modulate uptake and growth of Legionella pneumophila in Dictyostelium discoideum. Microbiology, 150(9), 2825-2835.

50) Derré, I., & Isberg, R. R. (2004). Legionella pneumophila replication vacuole formation involves rapid recruitment of proteins of the early secretory system. Infection and immunity, 72(5), 3048-3053.

51) Peterson, J. W. (1996). Bacterial pathogenesis. In Medical Microbiology. 4th edition. University of Texas Medical Branch at Galveston.

52) Nagai, H., Kagan, J. C., Zhu, X., Kahn, R. A., & Roy, C. R. (2002). A bacterial guanine nucleotide exchange factor activates ARF on Legionella phagosomes. Science, 295(5555), 679-682.

53) Southwick, F. S., & Purich, D. L. (1998). Listeria and Shigella actin-based motility in host cells. Transactions of the American Clinical and Climatological Association, 109, 160.

54) Kotewicz, K. M., Ramabhadran, V., Sjoblom, N., Vogel, J. P., Haenssler, E., Zhang, M., ... & Isberg, R. R. (2017). A single Legionella effector catalyzes a multistep ubiquitination pathway to rearrange tubular endoplasmic reticulum for replication. Cell host & microbe, 21(2), 169-181.

55) English, A. R., Zurek, N., & Voeltz, G. K. (2009). Peripheral ER structure and function. Current opinion in cell biology, 21(4), 596-602.

56) Steiner, B., Swart, A. L., Welin, A., Weber, S., Personnic, N., Kaech, A., ... & Hilbi, H. (2017). ER remodeling by the large GTPase atlastin promotes vacuolar growth of Legionella pneumophila. EMBO reports, 18(10), 1817-1836.

57) Rapoport, T. A. (2007). Protein translocation across the eukaryotic endoplasmic reticulum and bacterial plasma membranes. Nature, 450(7170), 663-669.

58) Holthuis, J. C., & Menon, A. K. (2014). Lipid landscapes and pipelines in membrane homeostasis. Nature, 510(7503), 48-57.

59) Felix, R. (2005). Molecular regulation of voltage-gated Ca2+ channels. Journal of receptors and Signal Transduction, 25(2), 57-71.

60) Hetz, C. (2012). The unfolded protein response: controlling cell fate decisions under ER stress and beyond. Nature reviews Molecular cell biology, 13(2), 89-102.

61) Walter, P., & Ron, D. (2011). The unfolded protein response: from stress pathway to homeostatic regulation. Science, 334(6059), 1081-1086.

62) Ron, D., & Walter, P. (2007). Signal integration in the endoplasmic reticulum unfolded protein response. Nature reviews Molecular cell biology, 8(7), 519-529.

63) Martinon, F., Chen, X., Lee, A. H., & Glimcher, L. H. (2010). TLR activation of the transcription factor XBP1 regulates innate immune responses in macrophages. Nature immunology, 11(5), 411.

64) Janeway Jr, C. A., & Medzhitov, R. (2002). Innate immune recognition. Annual review of immunology, 20(1), 197-216.

65) Martinon, F., Chen, X., Lee, A. H., & Glimcher, L. H. (2010). TLR activation of the transcription factor XBP1 regulates innate immune responses in macrophages. Nature immunology, 11(5), 411.

66) Tam, A. B., Mercado, E. L., Hoffmann, A., & Niwa, M. (2012). ER stress activates NF-κB by integrating functions of basal IKK activity, IRE1 and PERK. PloS one, 7(10), e45078.

67) Chan, S. W. (2014). Unfolded protein response in hepatitis C virus infection. Frontiers in microbiology, 5, 233.

68) Roy, C. R., Salcedo, S. P., & Gorvel, J. P. E. (2006). Pathogen–endoplasmic-reticulum interactions: in through the out door. Nature Reviews Immunology, 6(2), 136-147.

69) Mehlitz, A., Karunakaran, K., Herweg, J. A., Krohne, G., van de Linde, S., Rieck, E., ... & Rudel, T. (2014). The chlamydial organism S imkania negevensis forms ER vacuole contact sites and inhibits ER-stress. Cellular microbiology, 16(8), 1224-1243.

70) de Jong, M. F., Starr, T., Winter, M. G., den Hartigh, A. B., Child, R., Knodler, L. A., ... & Tsolis, R. M. (2013). Sensing of bacterial type IV secretion via the unfolded protein response. MBio, 4(1).

71) Guimarães, E. S., Gomes, M. T. R., Campos, P. C., Mansur, D. S., Dos Santos, A. A., Harms, J., ... & Oliveira, S. C. (2019). Brucella abortus cyclic dinucleotides trigger STING-dependent unfolded protein response that favors bacterial replication. The Journal of Immunology, 202(9), 2671-2681.

72) Sherwood, R. K., & Roy, C. R. (2016). Autophagy evasion and endoplasmic reticulum subversion: the yin and yang of Legionella intracellular infection. Annual review of microbiology, 70, 413-433.

73) Kotewicz, K. M., Ramabhadran, V., Sjoblom, N., Vogel, J. P., Haenssler, E., Zhang, M., ... & Isberg, R. R. (2017). A single Legionella effector catalyzes a multistep ubiquitination pathway to rearrange tubular endoplasmic reticulum for replication. Cell host & microbe, 21(2), 169-181.

74) Treacy-Abarca, S., & Mukherjee, S. (2015). Legionella suppresses the host unfolded protein response via multiple mechanisms. Nature communications, 6(1), 1-10.

Chapter 2

Non-canonical activation of the ER stress sensor ATF6 by *Legionella pneumophila* effectors

Nnejiuwa U. Ibe,[1,2] **Shaeri Mukherjee**[1,2*]

[1]Department of Microbiology and Immunology, University of California, San Francisco, San Francisco, CA 94143, USA.

[2]George Williams Hooper Foundation, University of California, San Francisco, San Francisco, CA 94143, USA.

*Correspondence: shaeri.mukherjee@ucsf.edu (S.M.)

Abstract

The intracellular bacterial pathogen *Legionella pneumophila* (*L.p.*) secretes ~330 effector proteins into the host cell to sculpt an Endoplasmic Reticulum (ER)-derived replicative niche. We previously reported five *L.p.* effectors that inhibit IRE1, a key sensor of the homeostatic unfolded protein response (UPR) pathway. In this study, we discovered a subset of *L.p.* toxins that selectively activate the UPR sensor ATF6, resulting in its cleavage, nuclear translocation and target gene transcription without affecting other UPR sensors such as PERK. In a deviation from the conventional model, this *L.p.*-dependent activation of ATF6 does not require its transport to the Golgi or its cleavage by the S1P/S2P proteases. We believe that our findings highlight the unique regulatory control that *L.p.* exerts upon the three UPR sensors and expand the repertoire of bacterial proteins that selectively perturb host homeostatic pathways.

Introduction

Several intracellular pathogens, including *Legionella pneumophila (L.p.)*, expertly manipulate host cell function to create their replicative niche. *L.p.* uses the specialized Dot/Icm Type IVB secretion system (T4SS) to translocate roughly 300 bacterial effector proteins into the host cytosol (Berger & Isberg, 1993, Hubber & Roy, 2010, Isberg, O'Connor et al., 2009, Vogel, Andrews et al., 1998). Once deposited into the cytosol, the effectors target a vast array of host proteins and can influence diverse biological processes which permit the use of *L.p*. as a tool to uncover novel biological mechanisms. During infection, *L.p.* uses its effectors to prevent fusion of the *Legionella*-containing vacuole (LCV) with the host endosomal machinery. Instead these effectors facilitate the remodeling of the LCV into a compartment that supports pathogen replication (Marra, Blander et al., 1992, Roy, Berger et al., 1998, Wiater, Dunn et al., 1998). Though fusion with lysosomes is evaded during infection, there is substantial interaction between the LCV and other host organelles including the endoplasmic reticulum (ER) (Horwitz & Silverstein, 1983, Swanson & Isberg, 1995, Tilney, Harb et al., 2001).

The ER-LCV interactions take on different forms as LCV maturation progresses. *L.p.* induces tubular ER rearrangements and intercepts ER-derived vesicles destined for the Golgi early in infection (Kotewicz, 2017). However, the mature LCV is studded with ribosomes and reticular ER proteins presenting a vacuolar environment that is substantially different and highlights the complexity of interactions between the ER and LCV. The ER serves as a critical regulatory site for protein and membrane lipid biosynthesis, and imbalances in protein load or membrane lipid perturbations can disrupt

many of its vital homeostatic functions (Rapoport, 2007, Halbleib, 2017). The unfolded protein response (UPR) serves as a prominent regulatory pathway that has been shown to respond to the burden of accumulating unfolded or misfolded proteins in the ER (Ron & Walter, 2007). In mammalian cells, the UPR is coordinated by three ER-localized transmembrane proteins, inositol-requiring protein-1 (IRE1), protein kinase RNA (PKR)-like ER kinase (PERK) and activating transcription factor-6 (ATF6), each of which initiate pathways designed to modulate the cellular response (Cox, Shamu et al., 1993, Lee, Tirasophon et al., 2002, Mori, Ma et al., 1993).

ATF6 is a type II transmembrane protein that is retained in the ER under normal homeostatic conditions through interactions with the resident chaperone BiP/GRP78 (Shen, Chen et al., 2002). Upon accumulation of unfolded proteins, the ER stress stimulates ATF6 translocation from the ER to the Golgi. At the Golgi, ATF6 is sequentially cleaved first by site-1 protease (S1P) in the luminal domain, then by site-2 protease (S2P) liberating the cytosolic ATF6-N terminal fragment, ATF6(NT) (Shen & Prywes, 2004, Ye, Rawson et al., 2000). Once cleaved, ATF6(NT) is recruited to the nucleus where it binds to cis-acting ER stress response elements (ERSE) in the promoter region of UPR target genes (Kokame, Kato et al., 2001, Yoshida, Okada et al., 2000). ATF6 activation is thought to facilitate cytoprotective adaptation to ER stress through the regulation of genes that improve protein folding and processing in the ER. ATF6 has been shown to suppress the UPR-induced apoptotic program once the stress is resolved (Wu et al., 2007), highlighting the pro-survival contributions of this signaling network.

Studies emphasizing cross talk between the UPR and bacterial infection have revealed an interconnectedness of ER stress-sensing and pathogen-sensing mechanisms in the cell (Li, Wang et al., 2011, Urano, Wang et al., 2000). Pathogenic perturbations endured during infection can impact ER homeostasis in a manner that can also induce ER stress responses. Intracellular pathogens across all kingdoms, from viruses to protozoans, have devised strategies to subvert or utilize one or more UPR program to benefit survival and replication within the host (Celli & Tsolis, 2015, Galluzzi, Diotallevi et al., 2017, Verchot, 2016). As further evidence, studies have demonstrated pathogen-mediated targeting of ATF6 can be beneficial for survival (Ambrose & Mackenzie, 2013, Hou, Dong et al., 2019, Hou, Wei et al., 2017) and replication (Yoshikawa, Sugimoto et al., 2020). Our previous analysis on *L.p.* mediated manipulation of the UPR revealed a dynamic reduction in full-length ATF6 protein levels during infection (Treacy-Abarca & Mukherjee, 2015). To further understand the relationship between *L.p.* infection and ATF6 processing, we sought to understand the mechanism by which *L.p.* modulates the ATF6 pathway. Here, we present evidence of a unique, non-canonical mode of ATF6 activation by *L.p.* that does not rely on host proteins that were previously thought to be essential for ATF6 activation. Surprisingly, we discover novel *L.p.* effectors that play a role in activation of ATF6 during infection.

Results

Proteasome-dependent degradation pathways are not required for ATF6 loss during *L.p.* infection

Upon infection with wild type *L.p.* (*WT-L.p.*), we observed near complete processing of endogenous full length ATF6 (**Figure 2.1**). The level of processing was similar to that

induced by the strong reducing agent and non-specific ER stress inducer, dithiothreitol (DTT) (**Figure 2.1**). An isogenic strain of *L.p.* that lacks a functional secretion system (Δ*dotA*-*L.p.*) was unable to downregulate ATF6 protein levels, suggesting that one or more bacterial effectors could be responsible for its targeting (**Figure 2.1**). Processing of ATF6 through regulated intramembrane proteolysis (RIP) by the S1P and S2P proteases has been studied extensively (Okada, 2003; Ye, 2000), yet degradative processing events have also been shown to control ATF6 levels even in the absence of ER stress (Hong, Li et al., 2004, Horimoto, Ninagawa et al., 2013). Interestingly, protein synthesis attenuation during *L.p.* infection has been shown to influence the IRE-1 branch of the UPR (Hempstead, 2015, Treacy-Abarca, 2015); but its impact on ATF6 has not been elucidated.

To test if proteasomal degradation contributed to the observed loss of ATF6, we monitored ATF6 processing in the presence or absence of proteasome inhibition, under conditions of protein synthesis arrest, or during *L.p.* infection. HEK293 cells stably expressing the Fcγ receptor (HEK293-FcγR) (to allow for antibody-mediated opsonization of *L.p.*) were pre-treated for 3 hours with the proteasome inhibitor MG-132 or control media. ER stress induction using DTT led to rapid ATF6 processing after 1 hour, whereas prolonged exposure to DTT for 3 hours resulted in recovery of ATF6 signal due to autoregulatory feedback from UPR induction (**Figure 2.1**). In contrast to UPR induction, cells treated with protein synthesis inhibitor cycloheximide (CHX) showed loss of full-length ATF6 signal after 3 hours post-treatment (**Figure 2.1**). While CHX treatment alone resulted in reduced levels of ATF6, pre-treatment with MG-132 stabilized ATF6 in the presence of CHX to pre-treatment levels (**Figure 2.1**), consistent with previously described observations (Haze et al., 1999). We next tested whether proteasomal inhibition could

stabilize ATF6 protein levels in cells infected with *WT-L.p.* or *ΔdotA-L.p.* strains (**Figure 2.1**). Similar to UPR induction using DTT (**Figure 2.1**), MG-132 treatment did not protect ATF6 from processing during WT *L.p.* infection (**Figure 2.1**). When cells were infected with *ΔdotA L.p.,* ATF6 remained at pre-infection levels and treatment with MG-132 did not have a significant impact (**Figure 2.1**). Previous studies have identified ATF6 as an ER-associated degradation (ERAD) substrate that undergoes constitutive degradation mediated by SEL1L (Horimoto et al., 2013). It was shown that ATF6 is a short-lived protein with a half-life less than 2 hours and the stability of ATF6 can be markedly increased by *Sel1L* disruption (Horimoto et al., 2013). To test if Sel1L dependent ERAD contributes to loss of ATF6 during infection, we next compared ATF6 processing in HEK293-FcγR cells that were treated with non-targeting or *SEL1L*-targeting siRNA. SEL1L knock-down led to an increase in ATF6(FL) levels by 1.5-fold in samples not treated with CHX (**Figure 2.1**). Similarly, while CHX treatment for 2 hours caused a reduction in ATF6(FL) levels in non-targeting siRNA cells, ATF6(FL) levels were again increased by 1.5-fold in *SEL1L* knock-down cells (**Figure 2.1**). However, there was no significant increase in ATF6(FL) signal intensity under *L.p.* infection when normalized to loading controls (**Figure 2.1**). As *L.p.* infection causes downregulation of protein synthesis (Belyi, Niggeweg et al., 2006, Fontana, Banga et al., 2011, Tzivelekidis, Jank et al., 2011), we considered this deregulation might contribute to loss of ATF6 during infection. To evaluate the impact of protein synthesis inhibition, we tested ATF6 processing in a *L.p.* strain lacking T4SS effectors that are known to block protein synthesis; Δ7-Translation *(Δ7-Trans-L.p.*) (Barry, Fontana et al., 2013, Fontana et al., 2011). Consistent with our previous results, we observed ATF6 processing to similar levels under infection using the *Δ7-Trans-L.p.* strain as seen with *WT-L.p.* (Figure

2.1). Together, these experiments suggest ATF6 processing during *L.p.* infection is not a direct result of enhanced proteasomal degradation or a consequence of protein synthesis arrest.

L. p. induces ATF6-mediated gene induction

We next considered how ATF6 processing affected its distal function as a nuclear transcription factor. To evaluate transcriptional activation, we used RT-qPCR to compare mRNA levels of ATF6 target genes, including UPR regulator/ER chaperone *BiP (HSPA5)*, in HEK293-FcγR cells under conditions of ER stress and *L.p.* infection. UPR induction with DTT increased expression of ER quality control genes *BiP* and *HERPUD1* by greater than 5-fold compared to control (DMSO-treated) cells (Figure 2.2). Interestingly, these ATF6-regulated genes were also induced in wild-type infected cells by greater than five-fold. When compared to protein synthesis inhibition using CHX, we found CHX did not induce *BiP* gene expression (**Figure 2.2**). To gain more insight into ATF6 induction patterns during *L.p.* infection, we examined the gene activation profile of *BiP* over the course of infection. Analysis of *BiP* mRNA expression using RT-qPCR indicated a spike in *BiP* expression between 4-5 hours post DTT treatment (**Figure 2.2**). When the expression profile was examined under avirulent *ΔdotA-L.p.* infections, *BiP* expression spiked between 1-3 hours post-infection, but quickly dropped to pre-infection levels by 5 hours post-infection. In contrast, infection with wild-type *L.p.* stimulated *BiP* expression around 3 hours post-infection, with pronounced gene induction even after 5 hours post-infection. The results were corroborated when ATF6 processing was monitored over the same time period. As shown previously, ATF6 is rapidly cleaved under DTT treatment (30 minutes),

but the ATF6(FL) signal recovers after sustained stress due to autoregulatory feedback (**Figure 2.2**). In comparison, *ΔdotA-L.p.* infection did not induce significant changes in ATF6(FL) levels over the course of infection (**Figure 2.2**). Yet, the appearance of a cleavage product at 1 hour correlated with the spike in *BiP* mRNA expression (**Figure 2.2**). When monitoring ATF6 processing under wild-type *L.p.* infection, the ATF6 processing profile also correlated with the changes in *BiP* mRNA expression. ATF6 signal intensity at 1-hour post-infection was approximately 90% of pre-infection levels (**Figure 2.2**). Within 3 hours of infection, the ATF6 signal intensity had decreased by roughly 50%. By 5 hours post-infection, *BiP* mRNA levels peaked and the ATF6 signal intensity dropped below 25% of pre-infection levels. In contrast to pharmacological ER stress induction, the loss of ATF6(FL) signal persisted throughout the infection. Taken together, the gene expression changes and ATF6 processing analysis demonstrate activation of the ATF6 pathway during *L.p.* infection. It is possible that *L.p.* could induce ATF6 downstream gene activation via effector(s) that don't require ATF6 cleavage. We thus determined whether ATF6 itself was required for UPR gene induction during infection. The ATF6 gene was targeted for knockdown in HEK293-FcγR cells using siRNA achieving greater than 80% knockdown efficiency (**Figure 2.2**). Though ATF6 knockdown nearly ablated *BiP* induction using DTT, ATF6 knockdown under *L.p.* infection markedly reduced *BiP* mRNA induction, suggesting that the endogenous ATF6 cleavage is indeed being utilized to induce downstream gene activation. However, *BiP* mRNA levels were still elevated nearly 4-fold compared to chemical induction in the knockdown cells (**Figure 2.2**). The residual *BiP* induction in *WT-L.p*. infection could be the result of the remnant ATF6 produced from incomplete knockdown. An alternate scenario is that certain *L.p.* effectors might bypass the

requirement for ATF6 cleavage by directly inducing ATF6 gene activation, suggestive of a redundant strategy often employed by *L.p*. during infection. Taken together, the data suggest that *L.p.* infection stimulates ATF6 processing and targets gene induction.

L. p. induces a non-canonical ATF6 activation

L.p.'s vast effector repertoire permits its subversion of numerous host pathways (Alix, 2011, Cornejo, 2017, Noack, 2020). However, it remains unknown which aspects of ATF6 activation during infection are host-driven or effector-driven. To further understand the mechanism of ATF6 activation, we performed pharmacological inhibition of host pathways that are thought to be essential for ATF6 activation. First, we utilized Ceapin inhibitors that selectively block ATF6 activation by inhibiting its translocation to the Golgi (Gallagher, Garri et al., 2016, Gallagher & Walter, 2016). Treatment of cells with DTT resulted in processing of ATF6 (**Figure 2.3**) and a greater than 5-fold induction of *BiP* mRNA (**Figure 2.3**). In contrast, co-treatment of cells with DTT and Ceapin A7 (+A7) partially protected ATF6 from cleavage (**Figure 2.3**) and reduced gene activation of *BiP* by nearly 50%. As shown earlier, *WT-L.p.* infection alone for 6 hours leads to complete processing of ATF6 and strong induction of *BiP* mRNA. Yet surprisingly, pre-treatment with Ceapin A7 did not prevent processing of ATF6 by the *WT-L.p.* strain (**Figure 2.3**). Additionally, *BiP* mRNA persisted at levels similar to untreated infections. This result suggests that ATF6 translocation from the ER to the Golgi is not a pre-requisite step required for its processing during infection. *L.p.* is known to exploit ER-to-Golgi trafficking and individual effectors have been identified that can disrupt Golgi homeostasis (Mukherjee, Liu et al., 2011). As disrupted homeostasis could result in mis-localization of

Golgi proteins, the impact of direct inhibition of S1P on ATF6 activation was tested using the inhibitor PF-429242 (Lebeau, Byun et al., 2018). Inhibition of S1P proteolysis activity using PF-429242 (PF) in the presence of DTT resulted in the appearance of a slower migrating species of ATF6 at a higher molecular weight likely due to extensive glycosylation in the Golgi (**Figure 2.3**). Further validating S1P inhibition, *BiP* mRNA induction was reduced by nearly 80% compared to DTT treatment alone (**Figure 2.3**). Remarkably, S1P inhibition did not alter ATF6 processing in *WT-L.p.* infected cells, and *BiP* mRNA was induced to similar levels as in untreated infected cells (**Figure 2.3**). The cleavage of ATF6 during *L.p.* infection even in the presence of Ceapin A7 and S1P inhibition are suggestive of an alternative proteolytic mechanism induced by *L.p.*. Because the S1P protease was not required for *L.p.* induced ATF6 processing, we next tested whether the canonical cleavage sites were a prerequisite for cleavage. To test this, a construct harboring a point mutation at the ATF6 S1P cleavage site ATF6(R415A/R416A) was used (**Figure 2.3**). HEK293-FcγR cells transiently expressing GFP-ATF6(R415A/R416A) were treated with UPR inducer DTT or infected with *WT-L.p*. or *ΔdotA-L.p*. strains. DTT treatment indicated processing of full-length ATF6 was greatly impaired in the S1P cleavage site mutant construct compared to wild type ATF6 (**Figure 2.3**) with over 75% of ATF6 remaining after DTT treatment. Yet, processing of ATF6 constructs was not attenuated under *WT-L.p.* infection even in the absence of a functional S1P cleavage site (**Figure 2.3**). Cumulatively, the data suggests *L.p.* infection stimulates the ATF6 pathway through means that circumvent the requirement of canonical pathway components.

L. p. infection stimulates translocation of ATF6 to the nucleus

We next examined whether *L.p.* infection causes nuclear accumulation of ATF6. Using a previously validated N-terminal GFP fusion protein, GFP-ATF6, the canonical activation pathway as induced with DTT was monitored using live-cell time-lapse microscopy (Chen et al., 2002). HeLa cells stably expressing the Fc Gamma receptor (HeLa-FcγR) were co-transfected with GFP-ATF6 and Golgi marker GalT-RFP. DTT treatment caused a rapid translocation of ATF6 from the ER to the Golgi within 30 minutes, and ATF6 signal colocalized with the Golgi marker GalT-RFP (**Figure 2.4**). After 120 minutes of DTT treatment, the ATF6 signal was predominantly localized to the nucleus. We then monitored the ATF6 localization pattern during *L.p.* infection using JF-644-stained Halo-tagged *L.p.* strains (**Figure 2.4**) (Grimm, 2017). Analysis of time-lapse micrographs revealed an increase in nuclear signal intensity during *WT-L.p.* infection (**Figure 2.4**). Strikingly, ATF6 activation during *L.p.* infection did not produce the robust Golgi/perinuclear recruitment as seen with DTT induction (**Figure 2.4**). The ability of *L.p.* to activate ATF6 in a manner that bypasses a need for Golgi translocation further corroborates our S1P mutants and Ceapin A7 studies that showed that ATF6 processing does not occur at the Golgi during infection. As infection progresses, the LCV is remodeled from a plasma membrane derived vacuole to an ER-like compartment in a process that involves the recruitment of host ER proteins to the LCV and the disruption of ER-to-Golgi trafficking (Swanson, 1995, Tinley, 2001). When monitoring ATF6 localization, confocal microscopy revealed substantial recruitment of ATF6 to the LCV membrane at 6 hours post-infection with over 80% of LCVs marked positive for ATF6 (**Figure 2.4**). Whereas a majority of LCVs were marked positive for ATF6 in WT-*L.p.*, the recruitment required a functional Dot/Icm system as the *ΔdotA-L.p.* infected

cells exhibited ATF6 recruitment to approximately 30% of LCVs. These data support the hypothesis that ATF6 is activated through a non-canonical mechanism.

ATF6 activation is strain- and species-specific

The data presented here highlight a T4SS-dependent activation strategy requiring the translocation of *Legionella* effector proteins. Therefore, we sought to identify effector proteins capable of inducing ATF6 activation by identifying *Legionella* strains that fail to efficiently process ATF6. Genomic analysis of over 30 *Legionella* strains and species revealed largely non-overlapping effector repertoires (Burstein, Amaro et al., 2016); therefore, we sought to use a comparative approach to test for ATF6 processing in different *Legionella* strains and species. Four *Legionella* species – *Legionella pneumophila*, *Legionella micdadei* (*L. mic)*, *Legionella wadsworthii* (*L. wad*), and *Legionella longbeachae* (*L. lon*) – were tested in addition to *Legionella pneumophila* strains – *Philadelphia* str. (*WT L.p.-Phila* or *ΔdotA L.p.-Phila*), *Paris* str. (*L.p.-Paris*), *Lens* str. (*L.p.-Lens*), and *Serogroup 6* str. (*L.p.-SG6*). The *Legionella* species and strains were used to infect HEK293-FcγR cells and endogenous ATF6 processing was monitored by immunoblot. While majority of the species and strains tested recapitulated the ATF6 processing seen with wild type *L.p.*, both *Legionella wadsworthii* and *Legionella pneumophila Paris* str. showed greatly reduced ATF6 processing (**Figure 2.5**). To test whether the infection resulted in a functional *Legionella* containing vacuole (LCV), we next tested the recruitment of ubiquitin to the vacuole. Ubiquitination of the LCV has been seen as a hallmark of successful infection (Horenkamp, 2014). Whereas the *Legionella wadsworthii* strain failed to show ubiquitin recruitment, the

Paris strain exhibited a robust recruitment of ubiquitin-modified substrates around the LCV in the HEK293-FcγR cells as observed by immunofluorescence (**Figure 2.5**).

Comparative genomic analysis between the *Philadelphia* str. and *Paris* str. revealed 17 known *Philadelphia* str. effector proteins that were absent from *L.p. Paris* str. effector repertoire (**Figure 2.5**). To identify effectors capable of activating the ATF6 pathway, a previously validated HEK293T cell line comprising of a stably integrated tandem ER stress response element with regulatory control over Luciferase expression (HEK-ERSE-Luc) (Gallagher, Garri et al., 2016) was used (**Figure 2.5**). The 17 Myc-tagged effectors were transiently expressed into the HEK-ERSE-Luc cell line and screened for luciferase induction. UPR induction as caused by thapsigargin (Tg) treatment produced a greater than 6-fold induction of luciferase activity (**Figure 2.5**). Control vectors expressing WT-ATF6 and S1P/S2P-ATF6-null were also evaluated in the luciferase cell line. As reported previously (Ye et al., 2000), overexpression of ATF6 led to an increased basal level of activation producing a 4-fold increase in luciferase activity over control vector, whereas the cleavage-deficient ATF6 mutant did not lead to an increase in baseline luciferase activity. These data exclude the possibility that simply overexpressing an ER protein triggers ATF6 expression. Our assay revealed that expression of 11 of the 17 effectors did not increase luciferase activity as compared to the control vector. While *L.p. Philadelphia str.* effectors *lpg1948*, *lpg2523*, and *lpg2525* stimulated a 2-fold increase in luciferase activity, the effectors *lpg0519* and *lpg2131* produced a greater than 2-fold increase in luciferase activity when expressed individually (**Figure 2.5**). Together, these results indicated that multiple effectors possess the capacity to induce the ATF6 pathway. Most of the effectors identified in this screen had little or no known function assigned to them.

Lpg0519 localizes to the ER and activates ATF6

To experimentally validate the results from the screen, the ATF6 targeting effectors were transiently expressed in HEK293T cells and UPR activation was monitored by immunoblot. Upon Tg treatment, a reduction in endogenous ATF6 was observed by 2 hours (**Figure 2.5**). By 4 hours of Tg treatment, the level of endogenous ATF6 was restored (**Figure 2.5**). Downstream of ATF6, UPR induction through Tg treatment also resulted in elevated levels of BiP/GRP78 compared to untreated cells. More broadly, Tg treatment also stimulated PERK pathway activation (a transmembrane UPR sensor at the ER) as shown by elevated ATF4 levels after 4 hours. When compared to Tg treatment, cells transfected with the GFP control vector did not exhibit a reduction in ATF6 levels, and BiP and ATF4 levels were not increased compared to untreated cells (**Figure 2.5**). However, cells transfected with N-terminally tagged GFP-Lpg0519 exhibited a dramatic reduction in endogenous ATF6 levels (**Figure 2.5**). Further validating ATF6 activation, BiP levels were also elevated in GFP-Lpg0519 transfected cells. However, the levels of ATF4 were not elevated in Lpg0519 transfected cells. These results highlight the UPR pathway specificity by Lpg0519 in activating the ATF6 pathway without targeting the UPR more generally. To further characterize Lpg0519, we investigated its subcellular localization in mammalian cells. GFP-Lpg0519 was transiently transfected in U2OS cells, and then examined in live cells using confocal microscopy. Whereas the GFP control vector was uniformly distributed throughout the cell (**Figure 2.5**), Lpg0519 co-localized with the ER-marker mCherry-ER-3 (**Figure 2.5**). Together these data suggest that Lpg0519 localizes to the ER and has the capacity to specifically induce the cytoprotective branch of the UPR (ATF6) without affecting the apoptotic branch (PERK).

Discussion

The UPR represents a critical node for re-establishing ER homeostasis under perturbations caused by the accumulation of misfolded proteins. Importantly, the three branches of the UPR work synergistically to maximize the response, yet the modalities by which each sensor contributes to homeostatic restoration differ considerably (Ron & Walter, 2007). Of importance, the PERK and IRE1 pathways are also UPR components that integrate signals from pathogen-associated molecular patterns that enable cross-talk between the UPR sensors and host cell innate immunity responses to defend again pathogen invasion (Martinon, 2010, Janssens, Pulendran et al., 2014, Smith, 2018). Therefore, the targeted inactivation of IRE1- and PERK-mediated enhancement of cytokine production by *L.p.* likely contributes to pathogen survival. The ATF6 pathway has also been linked as a modulator of pro-inflammatory responses and ATF6 was shown to enhance NF-κB signaling in ER stressed macrophages (Rao, 2014). Paradoxically, multiple *L.p. effectors* have been identified that have the capability of activating this inflammatory response pathway (Losick, 2010, Ge, 2009).

As the ATF6 pathway is mainly associated with the production of chaperones, ERAD components and lipid synthesis enzymes, the pro-survival attributes associated with ATF6 activation make it an attractive target that might serve to benefit pathogen survival and replication. Especially with respect to *L.p.*, an attractive model to test in future studies would be to examine whether *L.p.* utilizes ATF6 for lipid synthesis to actively contribute to the growing membrane of the LCV during the course of the infection. Indeed, targeting of the ATF6 branch of the UPR has been utilized by protozoan, bacterial, and viral pathogens

alike, and has been shown to contribute to intracellular replication in each system (Celli & Tsolis, 2015, Galluzzi et al., 2017, Jheng, Lau et al., 2010). Studies involving viruses have reported on a strategic activation of the UPR as a means to repurpose the autophagic response to benefit the virus where ATF6 knockdown reduced viral loads (Hou et al., 2019, Sharma, Bhattacharyya et al., 2017). However, this differs drastically from what is seen under *L.p.* infection, as the autophagy pathway is downregulated in *L.p.* infection (Choy, 2012). While bacteria have been shown to modulate UPR activity, it is striking how *L.p.* differentially modulates the different arms of the UPR by inhibiting IRE1, while activating ATF6 (Hempstead, 2015, Treacy-Abarca, 2015).

In this work, we aimed to further characterize the molecular mechanisms governing ATF6 processing in response to *L.p.* infection. ATF6 protein levels are tightly regulated through constitutive degradation via SEL1L/HRD1 dependent ERAD in conditions absent of ER stress and the impact of the constitutive degradation is revealed most strikingly under conditions of protein synthesis arrest (Fonseca, 2010, Horimoto, 2013). *L.p.*-induced translational inhibition occurs via host and pathogen mediated mechanisms and has been documented to have an impact on UPR induction under infection (Hempstead, 2015, Treacy-Abarca, 2015). Thus, we considered constitutive degradation of ATF6 to be the source for the reduction in protein levels during infection. Yet, we found impaired SEL1L-dependent ERAD and pharmacological inhibition of proteasomal degradation failed to stabilize ATF6 protein levels during infection (**Figure 2.1**).

Though proteasomal degradation pathways are active, our data suggest that degradation of ATF6 is not a major contributor to the loss of ATF6 signal during *L.p.*

infection. Furthermore, our data revealed that reduction in ATF6(FL) protein levels correlated with the appearance of an ATF6 cleavage fragment during wild-type infections (**Figure 2.2**). We considered the hypothesis that ATF6 is processed to form an active transcription factor capable of increasing the expression of target genes. Indeed, we found ATF6-regulated genes to be expressed under infection, and silencing of ATF6 reduced target gene expression, directly linking the sensor to downstream transcriptional activation (**Figure 2.2**). Though many UPR genes are highly expressed during infection, the genes are not translated at the rates observed under ER stress (Hempstead, 2015, Treacy-Abarca, 2015).

We then determined host and pathogen components required for ATF6 activation under infection. To our surprise, the major host pathway components were dispensable for *L.p.* mediated activation. Blockage of ATF6 specific ER-to-Golgi translocation and inhibition of S1P/S2P proteolytic activity traditionally restrict ATF6 activation under ER stress, however, neither impacted *L.p.* induced pathway activation in terms of ATF6 processing and downstream gene activation (**Figure 2.3**). Using time-lapse microscopy, we observed *L.p.* infection stimulated nuclear recruitment of ATF6 without the preceding Golgi translocation observed under ER stress-induced activation. Furthermore, ATF6 was detected around the LCV at 6 hours post infection, suggesting a mechanism for direct recruitment to the pathogen vacuole (**Figure 2.4**). More so, the capacity for wild type *L.p.* infection to induce processing of S1P- and S2P-site null mutants suggests a potentially unique site of cleavage under infection. However, the instability of the ATF6-NT cleavage fragment has so far hindered our efforts to the identify the novel cleavage site.

Our observations that ATF6 activation required a functional T4SS and the lack of a dependency for canonical host factors on ATF6 activation suggested one or more *L.p.* secreted effectors were involved. Using a phylogenetic approach, we determined that the *L.p. Paris* strain lacks the capacity to cleave ATF6. In doing so, we were able to identify several effectors unique to the *L.p. Philadelphia* strain that, when expressed individually, increased expression of an ATF6 specific reporter (**Figure 2.5**). Though the *L.p. Paris* strain lacks effectors shown to cleave ATF6, we do not dismiss the potential for the *Paris* strain to also contain negative regulators of ATF6 cleavage which could contribute to the observed reduction in ATF6 activation. Taken together, our results are the first example of a bacterial pathogen that can activate the ATF6 pathway independently of host pathway factors. Future work on these newly identified effectors might elucidate novel mechanisms of ATF6 activation and has the potential to open up new paradigms by which intracellular pathogens manipulate the cytoprotective UPR sensor ATF6.

Materials and Methods

Bacterial strains

All *Legionella* strains were gifts from Craig Roy's laboratory at Yale University. *Legionella* strains used in this study were routinely cultivated on Charcoal Yeast Extract (CYE) agar. The *ΔdotA*, *ΔsidC-sdcA*, and IPTG-inducible Halo-expressing strains were derived from the parental *Lp01* strain. The *Δ2,3,4,6,7*, *Δ2,3,6,7*, *Δ2,3,6 L.p.* strains (O'Connor et al., 2011), and *Δ7-translation L. pneumophila* strain (Barry, 2013) were a gift from Russell Vance's lab and are thymidine auxotrophs derived from the *Legionella pneumophila serogroup* 1 Lp02 (Berger and Isberg, 1993) . *Legionella pneumophila Paris B1* strain was purchased from ATCC (ATCC 700833). Chloramphenicol (10 ug/mL), IPTG (0.1 mM), and thymidine (100 ug/mL) were added to CYE agar plates as needed. *L.p.* were harvested from 2-day heavy patches and used to infect cells.

Cell culture

HEK-293 FcγRII and HeLa FcγRII cells were obtained from Craig Roy's laboratory at Yale University. All cells were cultured in DMEM (Life Technologies) supplemented with 10% fetal bovine serum (FBS) at 37 °C and 5% CO_2. RAW 264.7 macrophages were cultured in Roswell Park Memorial Institute media (RPMI) (Corning) supplemented with 10% FBS at 37 °C and 5% CO_2. Cells were placed in poly-L-lysine–treated plates and grown to 90% confluency. Drug treatments were performed at final concentration, 200 nM Tg (Enzo Life Sciences, Farmingdale, NY), 1 mM DTT (Research Products International (RPI), Mt Prospect, IL), 300 μM 4-(2-aminoethyl)benzenesulfonyl fluoride (AEBSF) (Sigma-Aldrich, St. Louis, MO), 1 μM Pf-429242 (Sigma-Aldrich), 20 μM MG-132 (Enzo Life Sciences), 25 μM

Cycloheximide (Sigma-Aldrich), 10 μM Ceapin A7 (Gallagher et al., 2016). Ceapin A7 was provided as a gift from the Peter Walter laboratory at UC San Francisco.

For transient transfections, cells were grown to 70% confluency and transfected with 2 μg of plasmid for 60 mm and 35 mm dishes, or 1 μg per well for 24-well plates using JetPRIME (Polyplus-transfection) according to the manufacturer's instructions. Cells were incubated with transfection reagent for 4 hours, then media replaced with fresh DMEM supplemented with 10% FBS. For siRNA transfections, cells were grown to 30-50% confluency and transfected using Oligofectamine (Thermo Fisher Scientific, Waltham, MA) according to the manufacturer's protocol. Cells were grown for 72 hours prior to application of treatment conditions. The following siRNA oligos used were purchased from Sigma-Aldrich: SEL1L-TTAACTTGAACTCCTCTCCCATAGA, Scramble-GCATACTCAACTACTTCGCATACTT; ATF6-GAACAGGGCTCAAATTCTC, Scramble-GCTAGTGCACAAGTACCTA.

Infection

Cells were infected at a multiplicity of infection (MOI) of 100 or 5. If cells required opsonization, *Legionella* polyclonal antibody (Invitrogen, Cat: PA1-7227) was used at 1:2,000 and incubated for 20 min at room temperature. Immediately after infection, cells were centrifuged for 5 min at 1,000 rpm. After centrifugation, cells were left at 37 °C for an additional 60 min. After 1 hour, cells were washed with 1x PBS to remove extracellular bacteria. DMEM supplemented with 10% FBS or the same media supplemented with treatment reagent was replaced after the washes in PBS. Infected cells were harvested at the designated times.

Quantitative RT–PCR

HEK-293 FCγ cell mRNA was harvested and isolated using Direct-zol™ RNA Miniprep Plus (Zymo Research, Irvine, CA) according to the manufacturer's protocol. cDNA synthesis was performed using QuantiTect Reverse Transcription Kit (Qiagen, Hilden, Germany) and cDNA reactions were primed with poly dT. Relative Quantitative PCR was performed using iTaq Universal SYBR Green Supermix (Bio-Rad, Hercules, CA). Endogenous GAPDH mRNA was used for normalization. Uninfected and untreated HEK-293 FCγRII cells were used as the endogenous control for each qPCR analysis. The following RT–qPCR primers were used: BiP (Human) forward- CATCACGCCGTCCTATGTCG, reverse- CGTCAAAGACCGTGTTCTCG; HERPUD1 (Human) forward- AACGGCATGTTTTGCATCTG, reverse- GGGGAAGAAAGGTTCCGAAG; Sel1l (Human) forward- AAACCAGCTTTGACCGCCAT, reverse- GTCATAGGTTGTAGCACACCAC; Hyou1 (Human) forward- GAGGAGGCGAGTCTGTTGG, reverse- GCACTCCAGGTTTGACAATGG; ATF6 (Human) forward- AGAGAAGCCTGTCACTGGTC, reverse- TAATCGACTGCTGCTTTGCC

Immunoblot analysis

Mammalian cells were lysed in Radioimmunoprecipitation assay buffer (RIPA) buffer with the addition of protease (Roche cOmplete), and phosphatase inhibitors (GB Sciences). Protein levels of lysates were determined using the BioRad DC/RC assay. Equal amounts of protein lysate were boiled with SDS load buffer, and equal amounts of protein were loaded. Immunoblotting was performed with the following antibodies: GAPDH (Proteintech, Cat: 60004-1-lg), ATF6 (Proteintech, Cat: 60004-1-lg), beta-Actin (Proteintech, Cat: 20536-1-AP), alpha-Tubulin (Proteintech, Cat: 66031-1-Ig), Sel1L (Abcam, Cat: ab78298), GFP tag

(Proteintech, Cat: 66002-1-Ig), BiP (Proteintech, Cat: 11587-1-AP), ATF4 (Cell Signaling Technology, Cat: 11815S) .

Immunofluorescence Microscopy

Cells were plated on 12 mm glass coverslips in 24-well plates. After 24 hours, cells were fixed, treated with drugs, or infected with *L.p.* as needed. For ubiquitin recruitment assay RAW cells were infected with *L.p.* at MOI = 5. 1 hour after infection, cells were washed twice with PBS to remove extracellular bacteria and incubated for 2 hours more. For co-localization assays, Cos7 cells were co-transfected with pcDNA-FcγRII (Arasaki, 2010) and GFP-ATF6α, then infected with *L.p.* at MOI = 10 and infected for 1, 4, or 8 hours. For 4- and 8-hour time points, cells were washed with PBS after 1 hour to remove extracellular bacteria. Coverslips were mounted with ProLong Diamond Antifade Mountant (Thermo Fisher Scientific) incubated at 37°C for 10 minutes, then imaged directly. For immunofluorescence, coverslips were washed with cold 1x PBS, fixed with 4% paraformaldehyde in PBS for 10 min at room temperature, permeabilized in 0.1% saponin in PBS, and blocked in 3% bovine serum albumin (BSA) in PBS, and then incubated with the appropriate primary and secondary antibodies diluted in 3% BSA. Nuclei were stained with Hoechst 33342 dye for 10 min before mounting on microscope slides. Coverslips were imaged using an inverted Nikon Eclipse Ti-E spinning disk confocal microscope equipped with a Prime 95B 25mm CMOS camera (Photometrics) camera. Antibodies used were Ubiquitin (Millipore, Cat: ST1200-100UG), and Secondary Antibody, Alexa Fluor 546 or Alexa Fluor 488 (Thermo Fisher Scientific).

Live Cell Microscopy

HeLa FcγRII cells expressing GFP-ATF6 were plated on 35 mm poly-lysine-coated imaging dishes (Cellvis, Mountain View, CA). Cells were infected at MOI = 5 with *WT*- or *ΔdotA L.p.* that were previously stained with HaloTag-Janelia Fluor 646 conjugates (Grimm et al., 2017). For staining, briefly, *L.p.* maintaining a HaloTag-expressing plasmid were harvested from a 2-day heavy patch and incubated at liquid culture overnight with 0.1 mM IPTG. Liquid culture at OD = 3.0 was then pelleted and resuspended in 5 mM Janelia Fluor 646 HaloTag ligand (JF646) in order to facilitate HaloTag-JF646 conjugation. After 15 min incubation with ligand in the dark, *L. pneumophila* were washed 1x with water. Stained bacteria were resuspended in 2 mL of DMEM lacking phenol red (Gibco) and used for infection of cells. Imaging of cells took place in a controlled chamber maintaining 37°C with 5% CO_2. A random selection of cells was imaged at 60X magnification at 5- or 10-minute intervals for 12 hours using a Nikon Eclipse Ti2 microscope with a Nikon DS-Qi2 camera. Cells that died or lost focus over the time course were omitted from analysis.

Luciferase assay

ONE-Glo Luciferase assay system was purchased from Promega. HEK-293T ERSE-Luciferase cells, provided as a gift from the Peter Walter laboratory at UC San Francisco and described previously (Gallagher et al. 2016), were seeded onto 6-well dishes at 70% confluency. Cells were transfected with Myc-tagged *Legionella* effectors as previously described (Barry, 2013) for 24 hours. Cells were suspended in 1mL DMEM and 50 uL aliquots were transferred to assay plate (Falcon, Cat:353296) in triplicate. One-Glo Luciferase reagent was pre-equilibrated to room temperature and added at equal volume

into each well. Assay plate measurements were performed on Tecan Saphire^2 with 1 s exposure. Background signal was subtracted from untreated untransfected cells. Treatment conditions were normalized to control Myc-tag expressing cells.

Quantification Statistical analysis

GraphPad Prism 6 software was used for statistical analysis. Where statistical analysis was performed an unpaired student's t-test was performed using three biological replicates. Statistical significance (*) was determined as a p-value < 0.05. Image analysis was performed using ImageJ.

Acknowledgements

We thank Dr. Philipp Schlaermann for doing preliminary studies on ATF6. We thank Peter Walter for scientific advice and for very generously providing us with the ERSE cell-line and Ceapin A7 inhibitor. We thank members of the Mukherjee lab for critical reading of the manuscript. S.M. is supported by the National Institutes of Health RO1 grant AI118974 and an award from the Pew Charitable Trust (A129837).

Author contributions

Conceptualization, S.M., N.U.I., Methodology, S.M and N.U.I.; Data Analysis, S.M. and N.U.I.; Investigation, N.U.I., Writing – Review & Editing, N.U.I., and S.M.; Funding Acquisition, S.M.; Resources, S.M.; Supervision, S.M.

Declaration of Interests

The authors declare no competing interests.

Figure 2.1

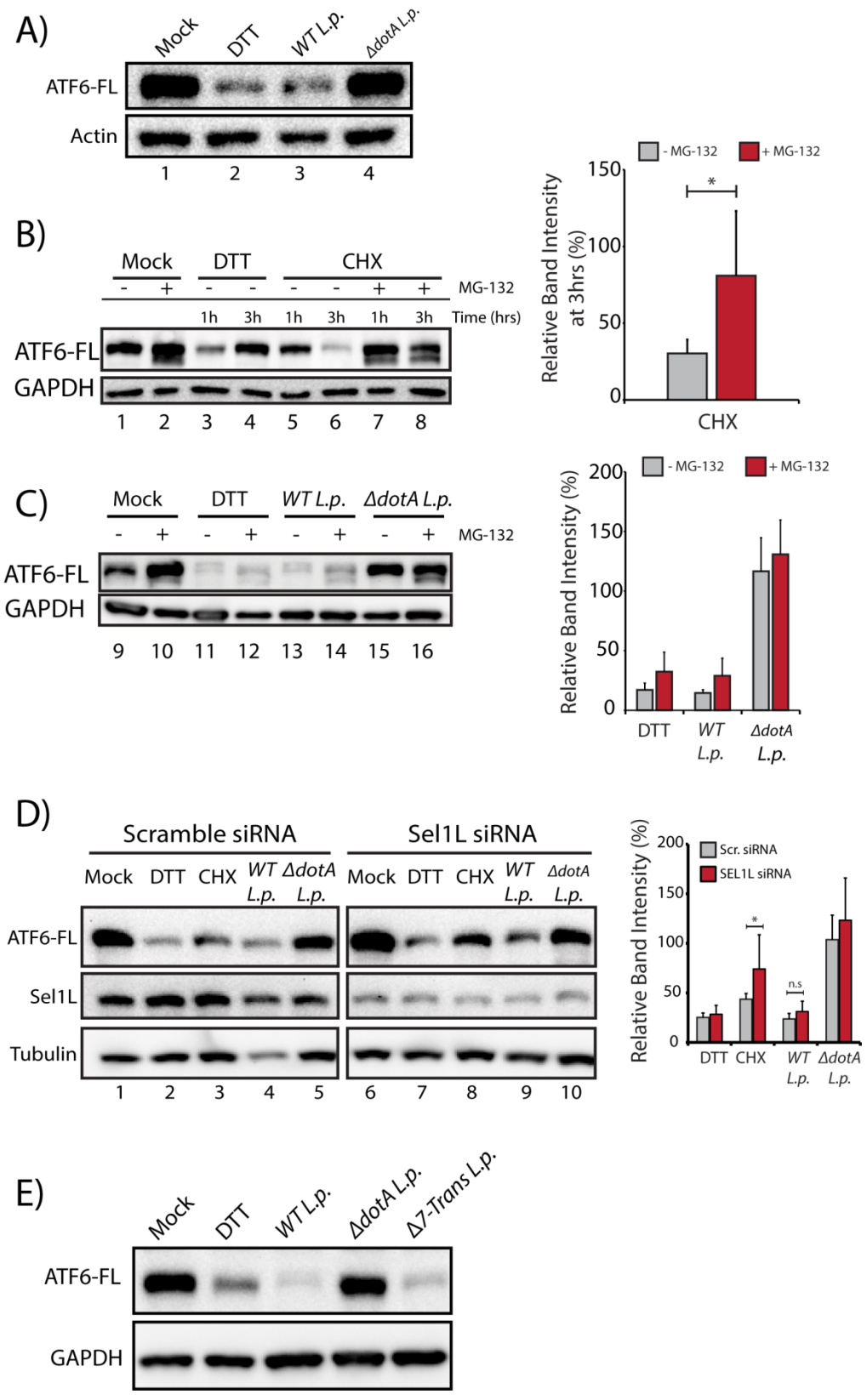
A)
Mock
DTT
WT L.p.
ΔdotA L.p.
ATF6-FL
Actin
1 2 3 4
B)
Mock
DTT
CHX
MG-132
Time (hrs)
ATF6-FL
GAPDH
1 2 3 4 5 6 7 8
- MG-132
+ MG-132
Relative Band Intensity at 3hrs (%)
CHX
C)
Mock
DTT
WT L.p.
ΔdotA L.p.
MG-132
ATF6-FL
GAPDH
9 10 11 12 13 14 15 16
Relative Band Intensity (%)
DTT
WT L.p.
ΔdotA L.p.
D)
Scramble siRNA
Sel1L siRNA
Mock DTT CHX WT L.p. ΔdotA L.p.
ATF6-FL
Sel1L
Tubulin
1 2 3 4 5 6 7 8 9 10
Scr. siRNA
SEL1L siRNA
n.s
E)
Mock
DTT
WT L.p.
ΔdotA L.p.
Δ7-Trans L.p.
ATF6-FL
GAPDH

Figure 2.1

***L.p.* infection induces ATF6 processing independently of proteasomal degradation and ERAD.**

(A) HEK293-FcγR cells were treated with 1 mM DTT for 1 hour or infected with *Legionella* pneumophila (*WT* or *ΔdotA*) for 6 hours prior to harvesting. Lysates were subjected to immunoblot analysis using anti-ATF6 and anti-Actin antibody. The precursor full-length ATF6 (ATF6-FL) fragment is shown.

(B and C) HEK293-FcγR cells were pre-treated with 20 uM MG-132 for 3 hours prior to indicated treatment conditions. (B) Cells were treated with 1mM DTT and 25 μM Cycloheximide (CHX) for 1 hour or 3 hours as indicated, or (C) infected with *WT*- or Δ*dotA*-*L.p.* for 6 hours (MOI = 5) and analyzed by immunoblot using anti-ATF6 and anti-GAPDH antibody. Quantitation from full length ATF6 signal from replicate experiments (n=3).

(D) Cell lysates from scramble or *SEL1L* siRNA-transfected HEK293-FcγR cells were analyzed by immunoblot using anti-ATF6, anti-Sel1L, and anti-Tubulin antibodies. CHX treatment was performed with 25 μM CHX for 2 hours. Quantitation from full length ATF6 signal from replicate experiments (n=3).

(E) HEK293-FcγR cells were treated with 1 mM DTT or infected with *WT L.p.*, *ΔdotA L.p.* and *Δ7-translation (Δ7-Trans) L.p.* strain as described in (A).

Figure 2.2

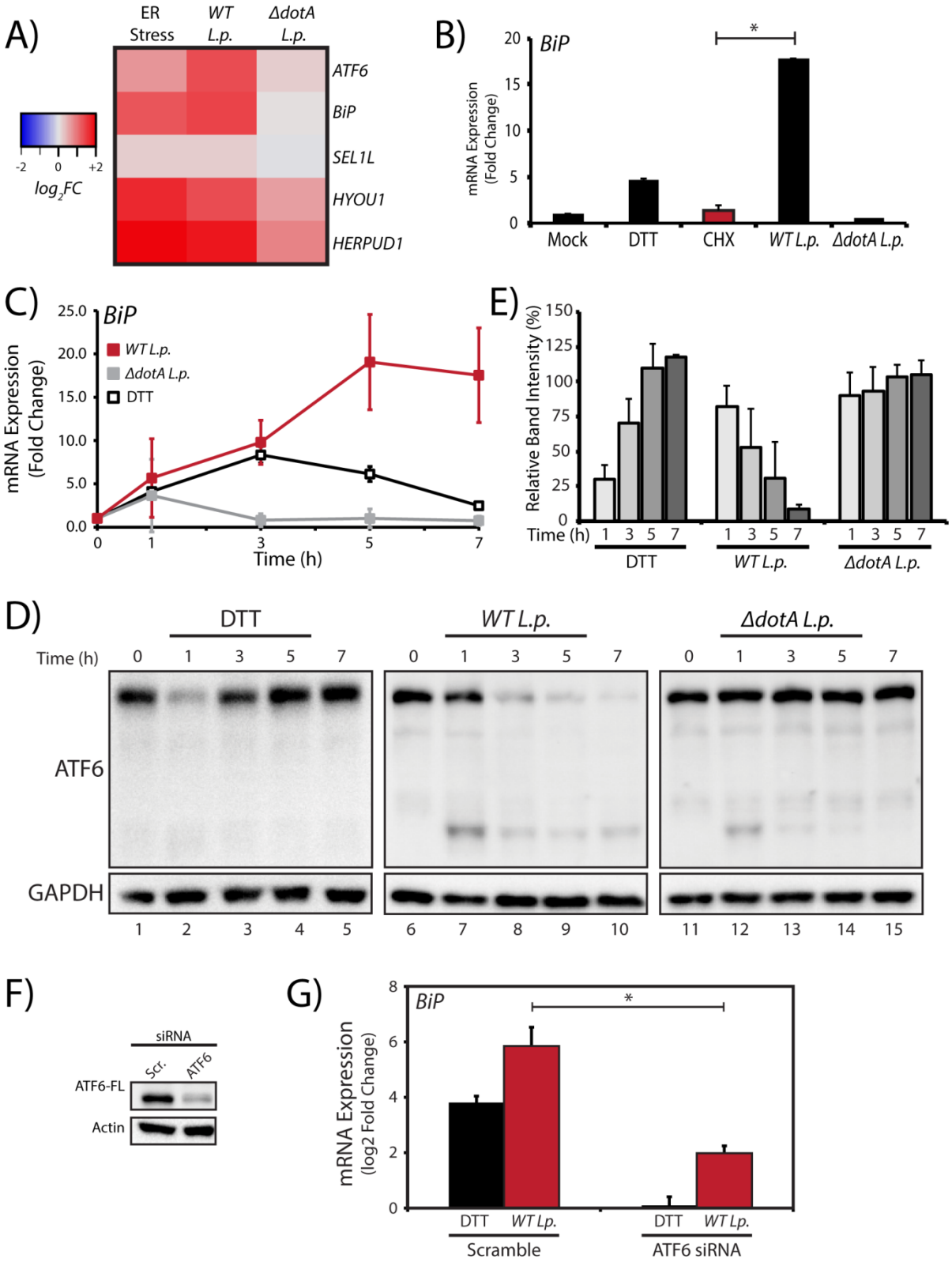
A)
ER Stress
WT L.p.
ΔdotA L.p.
ATF6
BiP
SEL1L
HYOU1
HERPUD1
-2 0 +2
log2FC
B)
BiP
mRNA Expression (Fold Change)
Mock
DTT
CHX
WT L.p.
ΔdotA L.p.
C)
BiP
WT L.p.
ΔdotA L.p.
DTT
mRNA Expression (Fold Change)
Time (h)
E)
Relative Band Intensity (%)
Time (h)
DTT
WT L.p.
ΔdotA L.p.
D)
DTT
WT L.p.
ΔdotA L.p.
Time (h)
ATF6
GAPDH
F)
siRNA
Scr.
ATF6
ATF6-FL
Actin
G)
BiP
mRNA Expression (log2 Fold Change)
DTT
WT Lp.
Scramble
ATF6 siRNA

Figure 2.2

***L.p.* infection stimulates ATF6 target gene induction.**
(A) HEK293-FcγR cells were treated with 1 mM DTT for 6 hours or infected with *L.p.* (*WT* or *ΔdotA*) for 6 hours prior to harvesting and RT-qPCR analysis using ER quality control genes *ATF6*, *BiP*, *SEL1L*, *HYOU1*, *HERPUD1*. Fold change shown relative to *GAPDH*.
(B) Cells were treated with 1mM DTT or 25 μM CHX for 6 hours, or infected with *L.p.* (*WT* or *ΔdotA*) for 6 hours. RT-qPCR analysis of *bip* was performed and fold change was calculated against GAPDH as a reference gene.
(C, D) *L.p.* infected HEK293-FcγR cells were harvested post- infection at indicated times, then (C) analyzed by RT-qPCR using primers against *bip,* or (D) lysed and analyzed by immunoblot using anti-ATF6 and anti-GAPDH antibodies. MOI = 100.
(E) Quantitation from full length ATF6 signal from replicate experiments relative time point 0 (n=3).
(F, G) *ATF6* siRNA or scramble siRNA transfected HEK293-FcγR cells were analyzed by (F) immunoblot using anti-ATF6 and anti-actin antibodies, or (G) analyzed by RT-qPCR using primers against *BiP*.

Figure 2.3

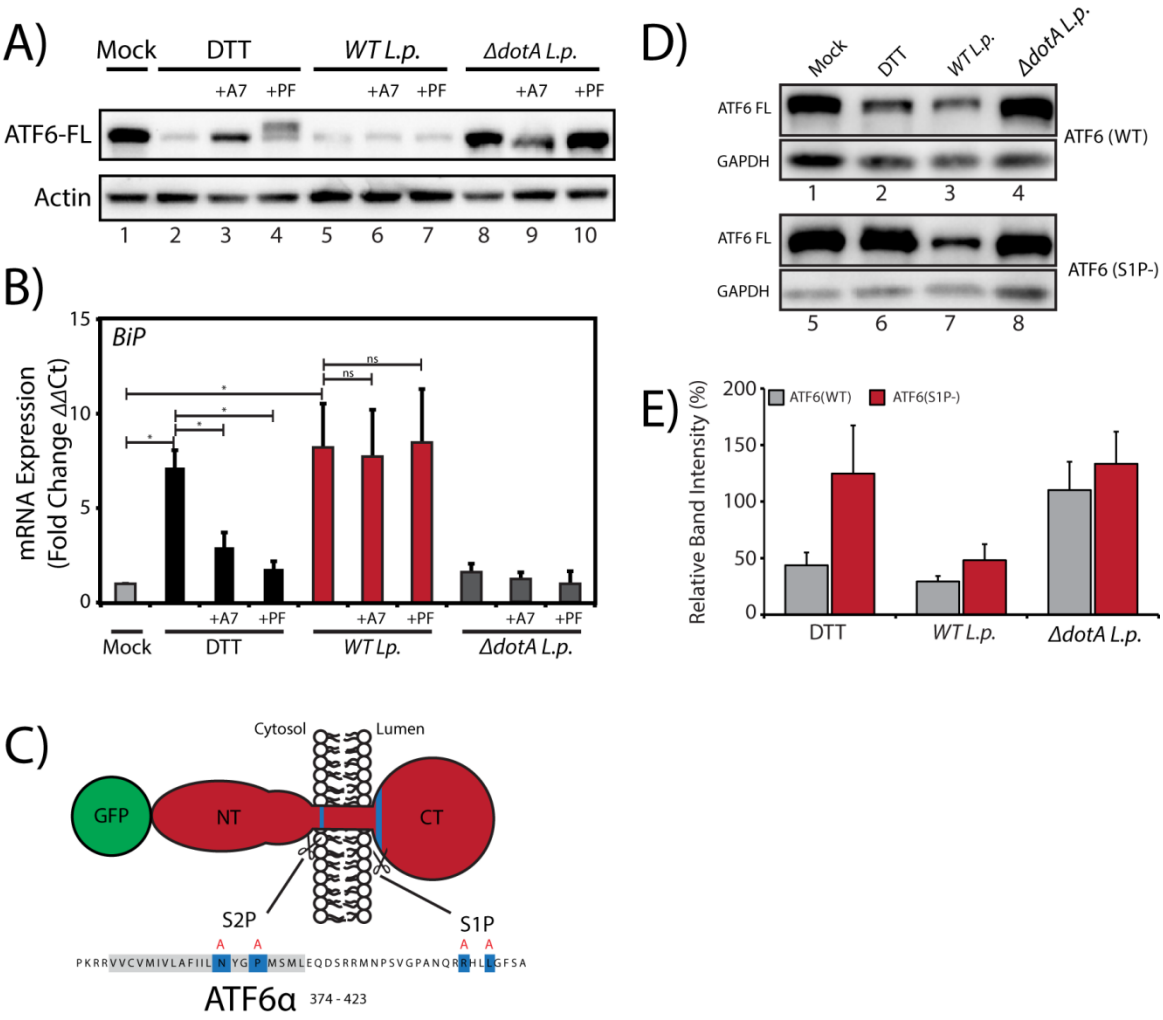
A)
Mock
DTT
WT L.p.
ΔdotA L.p.
+A7
+PF
ATF6-FL
Actin
1 2 3 4 5 6 7 8 9 10
B)
BiP
mRNA Expression (Fold Change ΔΔCt)
15
10
5
0
ns
Mock
DTT
WT Lp.
ΔdotA L.p.
C)
Cytosol
Lumen
GFP
NT
CT
S2P
S1P
PKRRVVCVMIVLAFIILNYGPMSMLEQDSRRMNPSVGPANQRRHLLGFSA
ATF6α 374 - 423
D)
Mock
DTT
WT L.p.
ΔdotA L.p.
ATF6 FL
GAPDH
ATF6 (WT)
ATF6 (S1P-)
1 2 3 4
5 6 7 8
E)
ATF6(WT)
ATF6(S1P-)
Relative Band Intensity (%)
200
150
100
50
0
DTT
WT L.p.
ΔdotA L.p.

Figure 2.3

***L.p.* induces non-canonical activation of ATF6.**
(A, B) HEK293-FcγR cells were treated 6 μM Ceapin A7 or 1 mM PF-429242 for 1 hour prior to infection or DTT treatment. DTT treated samples were incubated with 1 mM DTT for (A) 1 hour or (B) 4 hour. Infected cells were incubated with *L. p.* (*WT* or *ΔdotA*) for 6 hours, then lysed and (A) analyzed by immunoblot analysis using anti-ATF6 and anti-Actin antibody, or (B) analyzed by RT-qPCR using primers against *BiP*.
(C) Schematic of membrane bound N-terminal GFP-tagged ATF6 (red) with relevant features highlighting S1P and S2P cleavage site sequences (blue) and mutated residues for S1P and S2P cleavage site mutations (red letters).
(D) HEK293-FcγR cells were transfected with GFP-ATF6(WT) or GFP-ATF6(R415A/R416A). Transfected cells were incubated with 1 mM DTT for 1 hour, or infected with *L. p.* (*WT* or *ΔdotA*) for 6 hours and analyzed by immunoblot using anti-GFP and anti-GAPDH antibodies.
(E) Densitometry analysis showing the percentage of ATF6-FL signal remaining in treated cells relative to mock control cells.

Figure 2.4

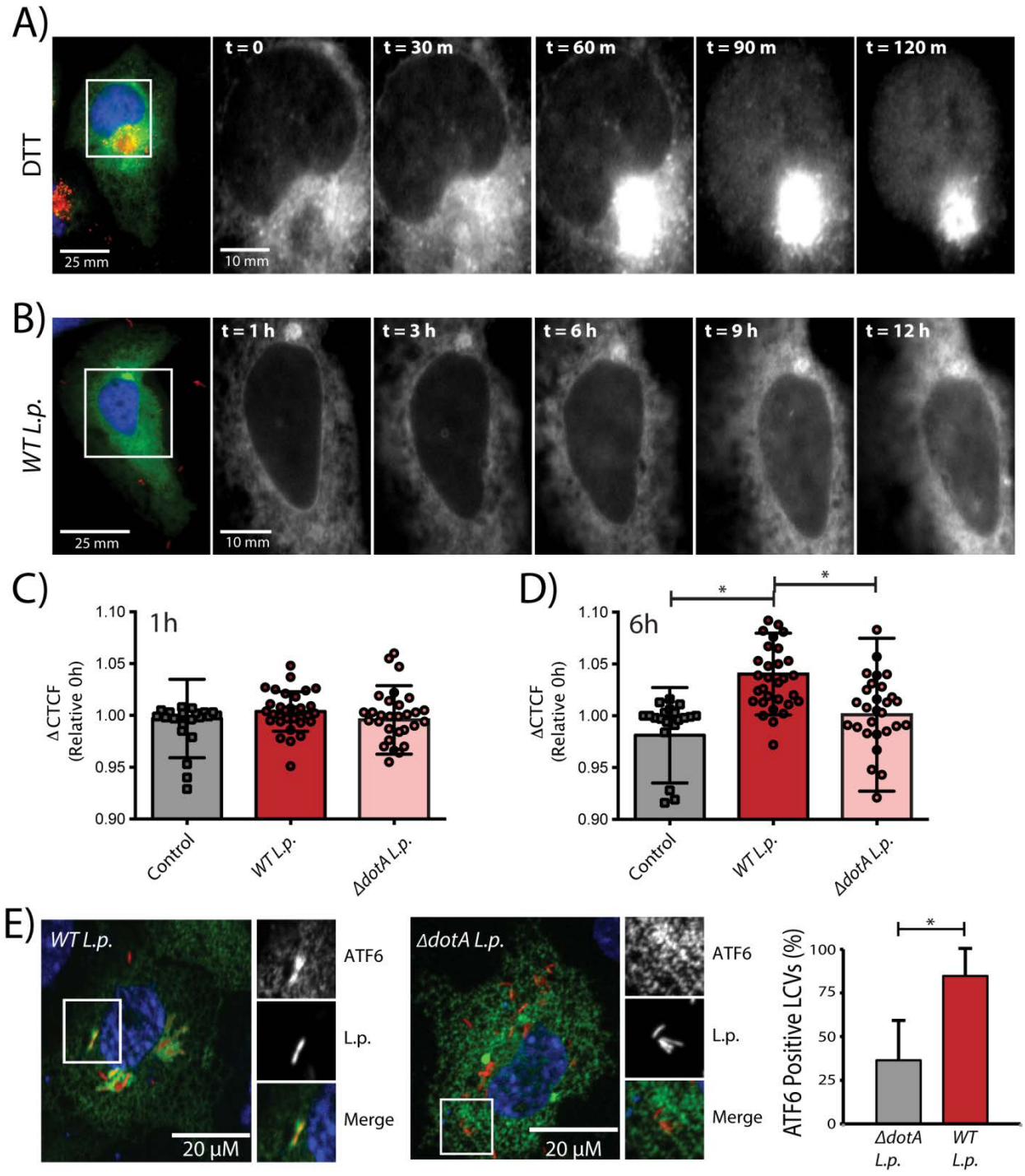
A)
DTT
t = 0
t = 30 m
t = 60 m
t = 90 m
t = 120 m
25 mm
10 mm
B)
WT L.p.
t = 1 h
t = 3 h
t = 6 h
t = 9 h
t = 12 h
25 mm
10 mm
C)
1h
ΔCTCF (Relative 0h)
1.10
1.05
1.00
0.95
0.90
Control
WT L.p.
ΔdotA L.p.
D)
6h
*
*
E)
WT L.p.
ATF6
L.p.
Merge
20 μM
ΔdotA L.p.
ATF6 Positive LCVs (%)
100
75
50
25
0
ΔdotA L.p.
WT L.p.

Figure 2.4

***L.p.* infection stimulates ATF6 nuclear recruitment.**

(A, B) Representative image stills from time-lapse wide-field fluorescent microscopy of HeLa-FcγR cells (A) transiently transfected with GalT-RFP and GFP-ATF6, then treated with 1 mM DTT or (B) transfected with GFP-ATF6, then infected with JF-646 stained *Halo-tag WT-L.p.* Live-cell epifluorescence image stills at timepoint 0 (t=0) (panel 1, scale bar = 25μm), with white box denoting location of inset. GFP-ATF6 signal (inset, panel 2-6, scale bar = 10 μm)

(C, D) Quantitation of temporal changes in nuclear localized GFP-ATF6 relative corrected total cell fluorescence (CTCF) of ATF6 in single cells followed over a 9-hour period analyzed between 1 hour (C) and 6 hours. Signal intensities analyzed from of control (n = 25), *WT L.p. (*n = 30*,)* or Δ*dotA L.p.* (n = 30) at designated time points were normalized to signal at 30 min post infection.

(E) Confocal micrographs of FcγRII and GFP-ATF6 transfected Cos7 cells infected with JF-646 stained *Halo-tag L. p. (WT or ΔdotA).* Values are the Mean ± SEM of three independent experiments in which at 50 LCVs were scored for each condition.

Figure 2.5

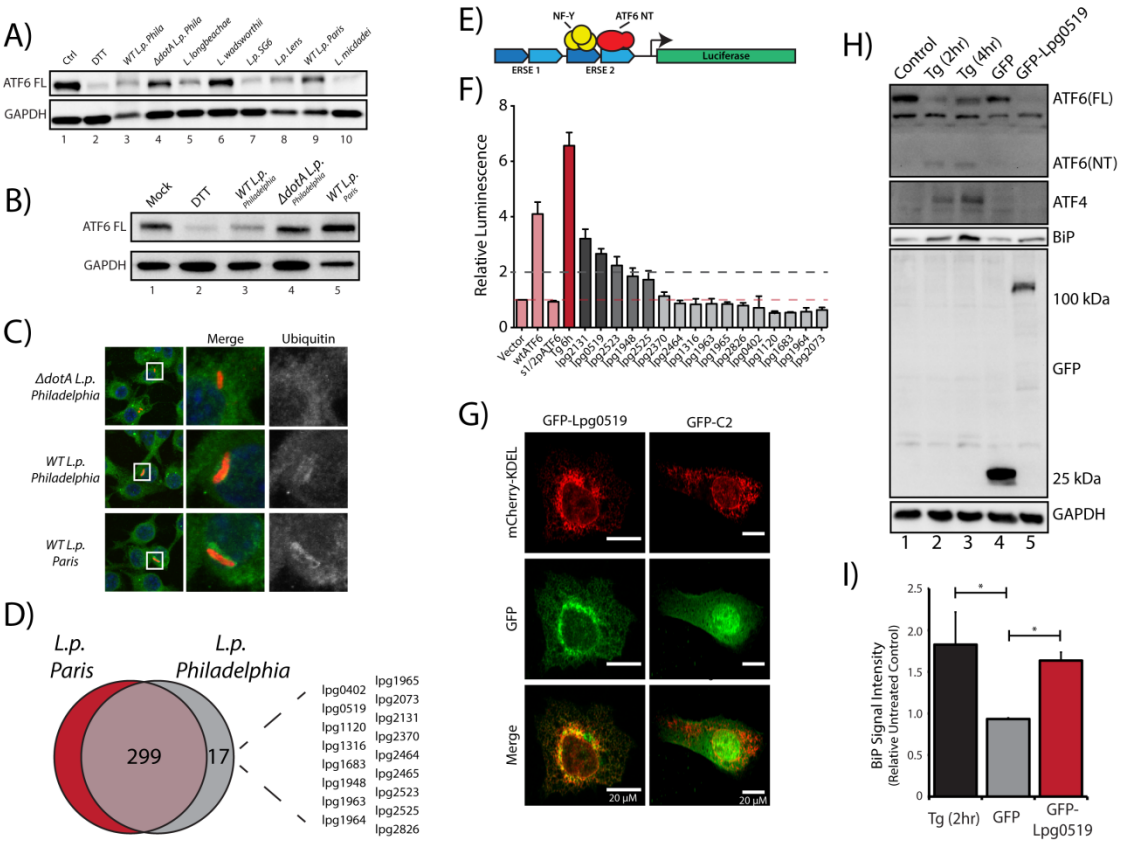
A)
Ctrl
DTT
WT L.p. Phila
ΔdotA L.p. Phila
L. longbeachae
L. wadsworthii
L.p. SG6
L.p. Lens
WT L.p. Paris
L. micdadei
ATF6 FL
GAPDH
1 2 3 4 5 6 7 8 9 10
B)
Mock
DTT
WT L.p. Philadelphia
ΔdotA L.p. Philadelphia
WT L.p. Paris
ATF6 FL
GAPDH
1 2 3 4 5
C)
Merge
Ubiquitin
ΔdotA L.p. Philadelphia
WT L.p. Philadelphia
WT L.p. Paris
D)
L.p. Paris
L.p. Philadelphia
299
17
lpg0402
lpg0519
lpg1120
lpg1316
lpg1683
lpg1948
lpg1963
lpg1964
lpg1965
lpg2073
lpg2131
lpg2370
lpg2464
lpg2465
lpg2523
lpg2525
lpg2826
E)
NF-Y
ATF6 NT
ERSE 1
ERSE 2
Luciferase
F)
Relative Luminescence
Vector
wtATF6
s1/2pATF6
lpg18h
lpg2131
lpg0519
lpg2523
lpg1948
lpg2525
lpg2370
lpg2464
lpg1316
lpg1963
lpg1965
lpg2826
lpg0402
lpg1120
lpg1683
lpg1964
lpg2073
G)
GFP-Lpg0519
GFP-C2
mCherry-KDEL
GFP
Merge
20 μM
H)
Control
Tg (2hr)
Tg (4hr)
GFP
GFP-Lpg0519
ATF6(FL)
ATF6(NT)
ATF4
BiP
100 kDa
GFP
25 kDa
GAPDH
1 2 3 4 5
I)
BiP Signal Intensity (Relative Untreated Control)
Tg (2hr)
GFP
GFP-Lpg0519

Figure 2.5

***L.p. Paris* strain does not induce ATF6 processing.**

(A, B) Immunoblots of HEK293-FcγR cells infected with *Legionella pneumophila* strains – *Philadelphia* str. (*WT L.p.-Phila* or *ΔdotA L.p.-Phila*), *Paris* str. (*L.p.-Paris*), *Lens* str. (*L.p.-Lens*), and *Serogroup 6* str. (*L.p.-SG-6*), and *Legionella micdadei* (*L. mic)*, *Legionella wadsworthii* (*L. wad*), and *Legionella longbeachae* (*L. lon*).

(C) Immunofluorescence micrographs from *L.p. (WT, dotA, or Paris str.)* infected HEK293-FcγR cells stained with Hoechst (blue) and antibodies against Ubiquitin (green) and *Legionella* (red).

(D) Identification of gene of orthologs of *L.p*. *Philadelphia* strain effectors through pairwise sequence alignments against *L.p. Paris* strain. Listed are *Philadelphia* strain effectors that are absent from the *Paris* strain.

(E) Schematic representation of ERSE-luciferase construct stably expressed in a HEK-293T based cell line (HEK293T-ERSE-Luciferase). Two copies of the ER stress response element (ERSE, blue) are cloned upstream of a minimal promoter driving Luciferase (green) gene expression. Once cleaved, ATF6(NT) binds the ERSE sequence and stimulates Luciferase expression.

(F) Primary screen data from ERSE-Luciferase reporter. HEK293T-ERSE-Luciferase cells were transiently transfected with Myc-tagged *Legionella* effectors or empty vector, GFP-ATF6(WT), or GFP-ATF6(R415A/R416A, N390F/P393L) (S1P/S2P). Treatments were internally normalized to non-treated control cells. Fold induction of luciferase activity from transfected samples taken relative to empty control vector transfected cells is charted. Baseline luciferase activity from control cells (red line) and 2-fold induction cutoff (grey line) are indicated.

(G) Confocal micrographs from U2OS cells transfected with GFP-C2 vector (right, center) or GFP-Lpg0519 (left, center) and mCherry-Calreticulin (red, top).

(H) Immunoblot of HEK293T cells treated with thapsigargin (Tg) for 2 hours or 4 hours, or transiently transfected with GFP-C2 vector or GFP-Lpg0519. Antibodies against ATF6, ATF4, BiP, GFP, and GAPDH were used.

(I) Quantification of replicate experiments (n=3) from (A) of BiP signal intensity relative non-treated control cells. Mean ± SEM, (*, $p < 0.05$).

References

1) Alix, E., Mukherjee, S., & Roy, C. R. (2011). Subversion of membrane transport pathways by vacuolar pathogens. Journal of Cell Biology, 195(6), 943-952.
2) Ambrose R.L., Mackenzie J.M. (2013) ATF6 signaling is required for efficient West Nile virus replication by promoting cell survival and inhibition of innate immune responses. Journal of virology 87: 2206-14
3) Arasaki, K., & Roy, C. R. (2010). Legionella pneumophila promotes functional interactions between plasma membrane syntaxins and Sec22b. Traffic, 11(5), 587-600.
4) Barry K.C., Fontana M.F., Portman J.L., Dugan A.S., Vance R.E. (2013) IL-1alpha signaling initiates the inflammatory response to virulent Legionella pneumophila in vivo. Journal of immunology 190: 6329-39
5) Belyi Y, Niggeweg R, Opitz B, Vogelsgesang M, Hippenstiel S, Wilm M, Aktories K (2006) Legionella pneumophila glucosyltransferase inhibits host elongation factor 1A. Proceedings of the National Academy of Sciences of the United States of America 103: 16953-8
6) Berger K.H., Isberg R.R. (1993) Two distinct defects in intracellular growth complemented by a single genetic locus in Legionella pneumophila. Molecular microbiology 7: 7-19
7) Burstein D, Amaro F, Zusman T, Lifshitz Z, Cohen O, Gilbert J.A., Pupko T, Shuman H.A., Segal G (2016) Genomic analysis of 38 Legionella species identifies large and diverse effector repertoires. Nature genetics 48: 167-75

8) Celli J, Tsolis RM (2015) Bacteria, the endoplasmic reticulum and the unfolded protein response: friends or foes? Nature reviews Microbiology 13: 71-82

9) Chen X, Shen J, Prywes R (2002) The luminal domain of ATF6 senses endoplasmic reticulum (ER) stress and causes translocation of ATF6 from the ER to the Golgi. The Journal of biological chemistry 277: 13045-52

10) Choy, A., Dancourt, J., Mugo, B., O'Connor, T. J., Isberg, R. R., Melia, T. J., & Roy, C. R. (2012). The Legionella effector RavZ inhibits host autophagy through irreversible Atg8 deconjugation. Science, 338(6110), 1072-1076.

11) Cornejo, E., Schlaermann, P., & Mukherjee, S. (2017). How to rewire the host cell: A home improvement guide for intracellular bacteria. Journal of Cell Biology, 216(12), 3931-3948.

12) Cox J.S., Shamu C.E., Walter P (1993) Transcriptional induction of genes encoding endoplasmic reticulum resident proteins requires a transmembrane protein kinase. Cell 73: 1197-206

13) Fagone P, Jackowski S (2009) Membrane phospholipid synthesis and endoplasmic reticulum function. Journal of lipid research 50 Suppl: S311-6

14) Fajardo M, Schleicher M, Noegel A, Bozzaro S, Killinger S, Heuner K, Hacker J, Steinert M (2004) Calnexin, calreticulin and cytoskeleton-associated proteins modulate uptake and growth of Legionella pneumophila in Dictyostelium discoideum. Microbiology 150: 2825-2835

15) Fonseca, S. G., Ishigaki, S., Oslowski, C. M., Lu, S., Lipson, K. L., Ghosh, R., ... & Urano, F. (2010). Wolfram syndrome 1 gene negatively regulates ER stress signaling in rodent and human cells. The Journal of clinical investigation, 120(3), 744-755.

16) Fontana M.F., Banga S, Barry K.C., Shen X, Tan Y, Luo Z.Q., Vance R.E. (2011) Secreted bacterial effectors that inhibit host protein synthesis are critical for induction of the innate immune response to virulent Legionella pneumophila. PLoS Pathog 7: e1001289

17) Gallagher C.M., Garri C, Cain E.L., Ang K.K., Wilson C.G., Chen S, Hearn B.R., Jaishankar P, Aranda-Diaz A, Arkin M.R., Renslo A.R., Walter P (2016) Ceapins are a new class of unfolded protein response inhibitors, selectively targeting the ATF6alpha branch. eLife 5

18) Gallagher C.M., Walter P (2016) Ceapins inhibit ATF6alpha signaling by selectively preventing transport of ATF6alpha to the Golgi apparatus during ER stress. eLife 5

19) Galluzzi L, Diotallevi A, Magnani M (2017) Endoplasmic reticulum stress and unfolded protein response in infection by intracellular parasites. Future science OA 3: FSO198

20) Gao L.Y., Susa M, Ticac B, Abu Kwaik Y (1999) Heterogeneity in intracellular replication and cytopathogenicity of Legionella pneumophila and Legionella micdadei in mammalian and protozoan cells. Microbial pathogenesis 27: 273-87

21) Ge, J., Xu, H., Li, T., Zhou, Y., Zhang, Z., Li, S., ... & Shao, F. (2009). A Legionella type IV effector activates the NF-κB pathway by phosphorylating the IκB family of inhibitors. Proceedings of the National Academy of Sciences, 106(33), 13725-13730.

22) Grimm, J. B., Muthusamy, A. K., Liang, Y., Brown, T. A., Lemon, W. C., Patel, R., ... & Lavis, L. D. (2017). A general method to fine-tune fluorophores for live-cell and in vivo imaging. Nature methods, 14(10), 987.

23) Haenssler E, Ramabhadran V, Murphy C.S., Heidtman M.I., Isberg RR (2015) Endoplasmic Reticulum Tubule Protein Reticulon 4 Associates with the Legionella pneumophila Vacuole and with Translocated Substrate Ceg9. Infection and immunity 83: 3479-89

24) Halbleib, K., Pesek, K., Covino, R., Hofbauer, H.F., Wunnicke, D., Hänelt, I., Hummer, G. and Ernst, R. (2017). Activation of the unfolded protein response by lipid bilayer stress. Molecular cell, 67(4), 673-684.

25) Haze K, Yoshida H, Yanagi H, Yura T, Mori K (1999) Mammalian transcription factor ATF6 is synthesized as a transmembrane protein and activated by proteolysis in response to endoplasmic reticulum stress. Molecular biology of the cell 10: 3787-99

26) Hempstead, A. D., & Isberg, R. R. (2015). Inhibition of host cell translation elongation by Legionella pneumophila blocks the host cell unfolded protein response. Proceedings of the National Academy of Sciences, 112(49), E6790-E6797.

27) Hong M, Li M, Mao C, Lee AS (2004) Endoplasmic reticulum stress triggers an acute proteasome-dependent degradation of ATF6. Journal of cellular biochemistry 92: 723-32

28) Horimoto S, Ninagawa S, Okada T, Koba H, Sugimoto T, Kamiya Y, Kato K, Takeda S, Mori K (2013) The unfolded protein response transducer ATF6 represents a novel transmembrane-type endoplasmic reticulum-associated degradation substrate requiring both mannose trimming and SEL1L protein. The Journal of biological chemistry 288: 31517-27

29) Horenkamp, F. A., Mukherjee, S., Alix, E., Schauder, C. M., Hubber, A. M., Roy, C. R., & Reinisch, K. M. (2014). Legionella pneumophila subversion of host vesicular transport by SidC effector proteins. Traffic, 15(5), 488-499.

30) Horwitz M.A., Silverstein SC (1983) Intracellular multiplication of Legionnaires' disease bacteria (Legionella pneumophila) in human monocytes is reversibly inhibited by erythromycin and rifampin. The Journal of clinical investigation 71: 15-26

31) Hou L, Dong J, Zhu S, Yuan F, Wei L, Wang J, Quan R, Chu J, Wang D, Jiang H, Xi Y, Li Z, Song H, Guo Y, Lv M, Liu J (2019) Seneca valley virus activates autophagy through the PERK and ATF6 UPR pathways. Virology 537: 254-263

32) Hou L, Wei L, Zhu S, Wang J, Quan R, Li Z, Liu J (2017) Avian metapneumovirus subgroup C induces autophagy through the ATF6 UPR pathway. Autophagy 13: 1709-1721

33) Hubber A, Roy C.R. (2010) Modulation of host cell function by Legionella pneumophila type IV effectors. Annu Rev Cell Dev Biol 26: 261-83

34) Isberg R.R., O'Connor TJ, Heidtman M (2009) The Legionella pneumophila replication vacuole: making a cosy niche inside host cells. Nature reviews Microbiology 7: 13-24

35) Janssens S, Pulendran B, Lambrecht BN (2014) Emerging functions of the unfolded protein response in immunity. Nature immunology 15: 910-9

36) Jeng E.E., Bhadkamkar V, Ibe N.U., Gause H, Jiang L, Chan J, Jian R, Jimenez-Morales D, Stevenson E, Krogan NJ, Swaney DL, Snyder MP, Mukherjee S, Bassik MC (2019) Systematic Identification of Host Cell Regulators of Legionella pneumophila

Pathogenesis Using a Genome-wide CRISPR Screen. Cell host & microbe 26: 551-563 e6

37) Jheng J.R., Lau K.S., Tang W.F., Wu M.S., Horng J.T. (2010) Endoplasmic reticulum stress is induced and modulated by enterovirus 71. Cellular microbiology 12: 796-813

38) Kokame K, Kato H, Miyata T (2001) Identification of ERSE-II, a new cis-acting element responsible for the ATF6-dependent mammalian unfolded protein response. The Journal of biological chemistry 276: 9199-205

39) Kotewicz, K.M., Ramabhadran, V., Sjoblom, N., Vogel, J.P., Haenssler, E., Zhang, M., Behringer, J., Scheck, R.A. and Isberg, R.R. (2017). A single Legionella effector catalyzes a multistep ubiquitination pathway to rearrange tubular endoplasmic reticulum for replication. Cell host & microbe, 21(2), 169-181.

40) Lebeau P, Byun J.H., Yousof T, Austin R.C. (2018) Pharmacologic inhibition of S1P attenuates ATF6 expression, causes ER stress and contributes to apoptotic cell death. Toxicology and applied pharmacology 349: 1-7

41) Lee K, Tirasophon W, Shen X, Michalak M, Prywes R, Okada T, Yoshida H, Mori K, Kaufman RJ (2002) IRE1-mediated unconventional mRNA splicing and S2P-mediated ATF6 cleavage merge to regulate XBP1 in signaling the unfolded protein response. Genes & development 16: 452-66

42) Li S, Wang L, Berman M, Kong YY, Dorf ME (2011) Mapping a dynamic innate immunity protein interaction network regulating type I interferon production. Immunity 35: 426-40

43) Losick, V. P., Haenssler, E., Moy, M. Y., & Isberg, R. R. (2010). LnaB: a Legionella pneumophila activator of NF-κB. Cellular microbiology, 12(8), 1083-1097.

44) Marra A, Blander S.J., Horwitz M.A., Shuman H.A. (1992) Identification of a Legionella pneumophila locus required for intracellular multiplication in human macrophages. Proceedings of the National Academy of Sciences of the United States of America 89: 9607-11

45) Martinon, F., Chen, X., Lee, A. H., & Glimcher, L. H. (2010). TLR activation of the transcription factor XBP1 regulates innate immune responses in macrophages. Nature immunology, 11(5), 411.

46) Mori K, Ma W, Gething M.J., Sambrook J (1993) A transmembrane protein with a cdc2+/CDC28-related kinase activity is required for signaling from the ER to the nucleus. Cell 74: 743-56

47) Mukherjee S, Liu X, Arasaki K, McDonough J, Galan JE, Roy CR (2011) Modulation of Rab GTPase function by a protein phosphocholine transferase. Nature 477: 103-6

48) Noack, J., & Mukherjee, S. (2020). "Make way": Pathogen exploitation of membrane traffic. Current Opinion in Cell Biology, 65, 78-85.

49) O'Connor, T. J., Adepoju, Y., Boyd, D., & Isberg, R. R. (2011). Minimization of the Legionella pneumophila genome reveals chromosomal regions involved in host range expansion. Proceedings of the National Academy of Sciences, 108(36), 14733-14740.

50) Okada, T., Haze, K., Nadanaka, S., Yoshida, H., Seidah, N. G., Hirano, Y., ... & Mori, K. (2003). A serine protease inhibitor prevents endoplasmic reticulum stress-induced

cleavage but not transport of the membrane-bound transcription factor ATF6. Journal of Biological Chemistry, 278(33), 31024-31032.

51) Omotade TO, Roy CR (2019) Manipulation of Host Cell Organelles by Intracellular Pathogens. Microbiology spectrum 7

52) Ragaz C, Pietsch H, Urwyler S, Tiaden A, Weber SS, Hilbi H (2008) The Legionella pneumophila phosphatidylinositol-4 phosphate-binding type IV substrate SidC recruits endoplasmic reticulum vesicles to a replication-permissive vacuole. Cellular microbiology 10: 2416-33

53) Rao, J., Yue, S., Fu, Y., Zhu, J., Wang, X., Busuttil, R. W., ... & Zhai, Y. (2014). ATF6 mediates a pro-inflammatory synergy between ER stress and TLR activation in the pathogenesis of liver ischemia-reperfusion injury. American Journal of Transplantation, 14(7), 1552-1561.

54) Rapoport T.A. (2007) Protein translocation across the eukaryotic endoplasmic reticulum and bacterial plasma membranes. Nature 450: 663-9

55) Robinson C.G., Roy C.R. (2006) Attachment and fusion of endoplasmic reticulum with vacuoles containing Legionella pneumophila. Cellular microbiology 8: 793-805

56) Ron D, Walter P (2007) Signal integration in the endoplasmic reticulum unfolded protein response. Nature reviews Molecular cell biology 8: 519-29

57) Roy C.R., Berger K.H., Isberg R.R. (1998) Legionella pneumophila DotA protein is required for early phagosome trafficking decisions that occur within minutes of bacterial uptake. Molecular microbiology 28: 663-74

58) Schroder M, Kaufman RJ (2005) The mammalian unfolded protein response. Annual review of biochemistry 74: 739-89

59) Schuelein R, Spencer H, Dagley L.F., Li P.F., Luo L, Stow J.L., Abraham G, Naderer T, Gomez-Valero L, Buchrieser C, Sugimoto C, Yamagishi J, Webb AI, Pasricha S, Hartland E.L. (2018) Targeting of RNA Polymerase II by a nuclear Legionella pneumophila Dot/Icm effector SnpL. Cell Microbiol 20: e12852

60) Sharma M, Bhattacharyya S, Sharma KB, Chauhan S, Asthana S, Abdin M.Z., Vrati S, Kalia M (2017) Japanese encephalitis virus activates autophagy through XBP1 and ATF6 ER stress sensors in neuronal cells. The Journal of general virology 98: 1027-1039

61) Shen J, Chen X, Hendershot L, Prywes R (2002) ER stress regulation of ATF6 localization by dissociation of BiP/GRP78 binding and unmasking of Golgi localization signals. Developmental cell 3: 99-111

62) Shen J, Prywes R (2004) Dependence of site-2 protease cleavage of ATF6 on prior site-1 protease digestion is determined by the size of the luminal domain of ATF6. The Journal of biological chemistry 279: 43046-51

63) Sherwood R.K., Roy C.R. (2016) Autophagy Evasion and Endoplasmic Reticulum Subversion: The Yin and Yang of Legionella Intracellular Infection. Annual review of microbiology 70: 413-33

64) Smith J.A. (2018) Regulation of Cytokine Production by the Unfolded Protein Response; Implications for Infection and Autoimmunity. Frontiers in immunology 9: 422

65) Swanson M.S., Isberg R.R. (1995) Association of Legionella pneumophila with the macrophage endoplasmic reticulum. Infection and immunity 63: 3609-20

66) Tilney L.G., Harb O.S., Connelly P.S., Robinson C.G., Roy C.R. (2001) How the parasitic bacterium Legionella pneumophila modifies its phagosome and transforms it into rough ER: implications for conversion of plasma membrane to the ER membrane. Journal of cell science 114: 4637-50

67) Treacy-Abarca S, Mukherjee S (2015) Legionella suppresses the host unfolded protein response via multiple mechanisms. Nat Commun 6: 7887

68) Tzivelekidis T, Jank T, Pohl C, Schlosser A, Rospert S, Knudsen C.R., Rodnina M.V., Belyi Y, Aktories K (2011) Aminoacyl-tRNA-charged eukaryotic elongation factor 1A is the bona fide substrate for Legionella pneumophila effector glucosyltransferases. PloS one 6: e29525

69) Urano F, Wang X, Bertolotti A, Zhang Y, Chung P, Harding H.P., Ron D (2000) Coupling of stress in the ER to activation of JNK protein kinases by transmembrane protein kinase IRE1. Science 287: 664-6

70) Verchot J (2016) How does the stressed out ER find relief during virus infection? Current opinion in virology 17: 74-79

71) Vogel J.P., Andrews H.L., Wong S.K., Isberg R.R. (1998) Conjugative transfer by the virulence system of Legionella pneumophila. Science 279: 873-6

72) Wiater L.A., Dunn K, Maxfield F.R., Shuman H.A. (1998) Early events in phagosome establishment are required for intracellular survival of Legionella pneumophila. Infection and immunity 66: 4450-60

73) Wu, J., Rutkowski, D. T., Dubois, M., Swathirajan, J., Saunders, T., Wang, J., ... & Kaufman, R. J. (2007). ATF6α optimizes long-term endoplasmic reticulum function to protect cells from chronic stress. Developmental cell, 13(3), 351-364.

74) Yamazaki, H., Hiramatsu, N., Hayakawa, K., Tagawa, Y., Okamura, M., Ogata, R., ... & Paton, J. C. (2009). Activation of the Akt-NF-κB pathway by subtilase cytotoxin through the ATF6 branch of the unfolded protein response. The Journal of Immunology, 183(2), 1480-1487.

75) Ye J, Rawson R.B., Komuro R, Chen X, Dave UP, Prywes R, Brown MS, Goldstein JL (2000) ER stress induces cleavage of membrane-bound ATF6 by the same proteases that process SREBPs. Molecular cell 6: 1355-64

76) Yoshida H, Okada T, Haze K, Yanagi H, Yura T, Negishi M, Mori K (2000) ATF6 activated by proteolysis binds in the presence of NF-Y (CBF) directly to the cis-acting element responsible for the mammalian unfolded protein response. Molecular and cellular biology 20: 6755-67

77) Yoshikawa Y, Sugimoto K, Ochiai Y, Ohashi N (2020) Intracellular proliferation of Anaplasma phagocytophilum is promoted via modulation of endoplasmic reticulum stress signaling in host cells. Microbiology and immunology

Chapter 3

Redundant targeting of the ATF6 pathway by *L.p.* translocated substrates

Introduction

L.p. uses over 300 secreted effectors to disrupt host cell processes to support bacterial replication within the cell. The substantial number of effector proteins that are translocated into the host during *L.p.* infection is considerably larger than other well studied intracellular bacterial pathogens. *L.p.* has nearly three times the number of *Coxiella sp*. secreted effectors (>100 effectors) and roughly 20 times the number of *Brucella sp*. secreted effectors (~15 effectors) [1, 2]. Once translocated, these effectors employ specialized mechanisms to disrupt, circumvent, or make use of a variety of host cellular pathways. Most intriguingly, the presence of a strikingly large number of translocated substrates permits multiple layers of regulation and redundancy in virulence strategies.

Studies involving *L.p.* have revealed the existence of multiple effector proteins that can modulate a single host protein. An example resides in the activities of the *L.p.* glucosyltransferases Lgt1-Lgt3 and SidI/SidL [3]. Amongst the characterized activities, the effectors can individually inhibit IRE1 mediated splicing of XBP1 in ER-stress treated cells when exogenously expressed, or during infection [4, 5]. Several instances of functional redundancy have also been observed, when multiple effectors target different components of the same pathway. For example, whereas the effector proteins Lgt1-3 inhibit translation through post-translational targeting of eukaryotic elongation factor eEF1A, the *L.p.* kinase

LegK4 exerts its inhibitory effect over translation through phosphorylation of the cytosolic chaperone Hsc70 [3, 6].

The previous chapter highlighted a non-canonical ATF6 activation strategy by *L.p.* that was coordinated by the multiple secreted effectors. From our analysis we highlighted activation of ATF6 by the *L.p.* effector Lpg0519 which was also shown to localize to the ER. Interestingly, our report also identified that the effector Lpg2131 was able to induce an ATF6-specific luciferase reporter by greater than two-fold. Additionally, effectors Lpg1948, Lpg2523, and Lpg2525 also stimulated luciferase induction by nearly two-fold. These findings highlight the potential for *L.p.* to redundantly target the ATF6 branch of the UPR through multiple effectors, yet the mechanisms by which they act remains unresolved. In this chapter, I introduce unpublished data that supports the existence of redundant ATF6 targeting mechanisms employed by *L.p.* during infection.

Identification of ATF6-targeted protease-like effectors

Our findings indicate ATF6 processing can occur independently of canonical proteases, membrane-bound transcription factor site-1 protease (S1P) and membrane-bound transcription factor site-2 protease (S2P) (see Chapter 2). As ATF6 processing occurred in the presence of S1P and S2P inhibition, we considered the possibility of *L.p.* effectors that can directly cleave ATF6. Using pairwise sequence analysis, we assessed the homology of known *L.p.* effectors to S1P and S2P as well as a comparison to the MEROPS database resource for peptidases [7]. From this search, we identified nine effectors with varying degrees of homology with a peptidase [Table 1]. Analysis of these effectors

revealed that overexpression of Lpg1960 resulted in a dramatic reduction in full length ATF6 levels [**Figure 3.1**].

We then considered if Lpg1960 could access the ER which would suggest the potential for direct interaction with ATF6. Using a GFP-tagged Lpg1960 construct, we monitored the localization pattern by fluorescence microscopy [**Figure 3.2**]. Whereas ER localized mCherry-KDEL exhibited a restricted ER localization pattern, Lpg1960 exhibited a dimorphic localization pattern with some cells showing a largely diffuse signal throughout the cytoplasm, while others showed a striking localization at the nucleus. Quantitation revealed that an equal percentage of cells exhibited cytoplasmic and nuclear localization under similar conditions (FIG3.2?). Importantly, when GFP-Lpg1960 expression was monitored via immunoblot, there was only a single band corresponding to the molecular weight of the full length GFP-Lpg1960 [**Figure 3.1**]. This suggested that the dimorphic localization pattern was not the product of post-translation processing.

We then sought to determine if Lpg1960 exhibited proteolytic activity. Lpg1960 was sub cloned into a GST-tagged construct to facilitate bacterial expression and GST-purification of the effector. To test for proteolytic activity, we monitored the cleavage potential of purified Lpg1960 against the model substrate casein. Co-incubation of casein with model protease Trypsin led to noticeable increase in cleaved casein products [**Figure 3.3**]. However, GST-Lpg1960 did not induce casein cleavage significantly above casein cleavage with GST alone. The results suggest Lpg1960 does not possess catalytic activity, however we cannot exclude the potential that accessory cofactors are required for the catalytic activity of Lpg1960.

ATF6-independent target gene induction under *L.p.* infection

Results from Chapter 2 suggested that ER-to-Golgi translocation and S1P/S2P-dependent cleavage were dispensable for ATF6 activation during *L.p.* infection. We then sought to determine if ATF6 target gene induction seen during *L.p.* infection was caused by the ATF6 sensor itself. To our surprise, target gene induction was dampened, but persisted under *L.p.* infection with siRNA knockdown of ATF6 [**Chapter 2**, **Figure 2.2**]. In contrast DTT-induced target gene induction was nearly completely attenuated under ATF6 siRNA knockdown. Though the residual target gene induction could be the result of incomplete knockdown, we considered how molecular mimicry through the use of *L.p.* effectors could stimulate ATF6 target gene induction. Further support for this hypothesis was the suggestive observation that the antibody against human ATF6 detects a single band in *L.p.* lysates [**Figure 3.4**].

ATF6 is a member of the leucine zipper family of proteins that can heterodimerize with the NF-Y transcription factor complex to bind the ER stress response element (ERSE) consensus sequence (5'-CCAAT-N9-CCAC[GA]-3') and ERSE II sequence (5'-ATTGG-N-CCACG-3') in the promoters of target genes [9]. To search for an ATF6-like *L.p.* effector, we performed a homology search of *L.p.* effectors against human ATF6. When the search criteria were restricted to the transcriptional activation domain of ATF6 (a.a. 1-150), the *L.p.* effector Lpg2519 was identified. To our surprise, Lpg2519 (SnpL) was characterized as a nuclear-localized effector which can upregulate host gene expression upon ectopic expression [8]. Using a GFP-tagged SnpL, we confirmed its nuclear localization when expressed in HeLa cells [**Figure 3.5**]. Through its DNA binding interaction to ERSE

sequences, when overexpressed, ATF6 can increase the basal expression levels of target genes, including *BiP* and *ATF6* itself [10]. However, our preliminary results did not reveal changes in ATF6 protein expression levels or BiP mRNA levels when Lpg2519 was overexpressed in HEK293T cells [**Figure 3.6**].

Conclusions and Future Work

Additional investigations into alternative ATF6 targeting mechanisms revealed that over-expression of a protease-like effector, Lpg1960, decreased ATF6 levels. When tested against the model protease substrate, casein, Lpg1960 failed to exhibit proteolytic activity. However, further investigation needs to be done to test for the requirement of additional cellular factors that enhance the catalytic activity of Lpg1960. Alternatively, Lpg1960 might exert its function on ATF6 indirectly. We also observed homology between the transactivation domain of ATF6 and the *L.p*. effector Lpg2519. Though Lpg2519 did not directly impact ATF6 protein levels, the effect on ATF6 target gene induction has not been explored. *L.p.* effectors Lpg1948, Lpg2131, Lpg2523, and Lpg2525 all stimulated an increase in an ATF6-specific luciferase reporter. However, toxicity associated with overexpression of these effectors has hampered further examination of their molecular modes of action. The use of low expression or inducible expression vectors might circumvent the toxicity restrictions that have precluded their examination.

Materials and Methods

Cell culture

HeLa FcγRII cells were obtained from Craig Roy's laboratory at Yale University. Cells were cultured in DMEM (Life Technologies) supplemented with 10% fetal bovine serum (FBS) at 37 °C and 5% CO_2. ER stress treatments were performed at final concentration, 200 nM Tg (Enzo Life Sciences, Farmingdale, NY) or 1 mM DTT (Research Products International (RPI), Mt Prospect, IL).

Transient transfections were performed in cells grown to 70% confluency and transfected with 2 μg of plasmid for 60 mm and 35 mm dishes, or 1 μg per well for 24-well plates using JetPRIME (Polyplus-transfection) according to the manufacturer's instructions. Cells were incubated with transfection reagent for 4 hours, then media replaced with fresh DMEM supplemented with 10% FBS.

Immunoblot analysis

Cells were lysed in Radioimmunoprecipitation assay buffer (RIPA) buffer with the addition of protease (Roche cOmplete), and phosphatase inhibitors (GB Sciences). Protein levels of lysates were determined using the BioRad DC/RC assay. Equal amounts of protein lysate were boiled with SDS load buffer, and equal amounts of protein were loaded. Immunoblotting was performed with the following antibodies: GAPDH (Proteintech, Cat: 60004-1-lg), ATF6 (Proteintech, Cat: 60004-1-lg), GFP tag (Proteintech, Cat: 66002-1-Ig), Myc (Proteintech, Cat: 16286-1-AP).

Live Cell Microscopy

HeLa FcγRII cells expressing GFP-Lpg1960 or co-expressing GFP-Lpg2519 and mCherry-KDEL were plated on 35 mm poly-lysine-coated imaging dishes (Cellvis, Mountain View, CA). A random selection of cells was imaged at 60X magnification using a Nikon Eclipse Ti2 microscope with a Nikon DS-Qi2 camera.

In-vitro Cleavage Assay

Protein samples were diluted to 0.1, 0.01, 0.001, and 0.0001 ug/uL with water to a final volume of 200 uL. Pierce™ Colorimetric Protease Assay Kit was used for in-vitro cleavage assay (Thermo Scientific Cat: 23263). Succinylated casein solution was added to treatment wells. Succinylated casein solution was replaced with Assay buffer for control treatments. The enzyme activity was measured using Magellan Tecan Saphire2 at 450 nm.

Quantitative RT–PCR

HEK-293 FCγ cell mRNA was harvested and isolated using Direct-zol™ RNA Miniprep Plus (Zymo Research, Irvine, CA) according to the manufacturer's protocol. cDNA synthesis was performed using QuantiTect Reverse Transcription Kit (Qiagen, Hilden, Germany) and cDNA reactions were primed with poly dT. Relative Quantitative PCR was performed using iTaq Universal SYBR Green Supermix (Bio-Rad, Hercules, CA). Endogenous GAPDH mRNA was used for normalization. Uninfected and untreated HEK-293 FCγRII cells were used as the endogenous control for each qPCR analysis. The following RT–qPCR primers were used: BiP (Human) forward- CATCACGCCGTCCTATGTCG, reverse- CGTCAAAGACCGTGTTCTCG

Table 3.1: Bioinformatically identified *Legionella* effectors with protease homology

***L.p*. Effector Protein**	**Protease Homology**
Lpg1110 (Lem5)	ATP-dependent Clp protease ATP-binding subunit ClpA
Lpg1111	Zinc Protease
Lpg1166	Rhomboid family intramembrane serine protease
Lpg1426 (VpdC)	ATP-dependent protease subunit HslV
Lpg1884 (LegC2/ylfB)	ATP-dependent protease/YifB protease family
Lpg1960 (LirA)	Zinc metalloprotease
Lpg1963 (PieA)	Zn-dependent protease
Lpg2131 (LegA6)	Zn-dependent protease
Lpg2444	Zinc metalloprotease

Figure 3.1

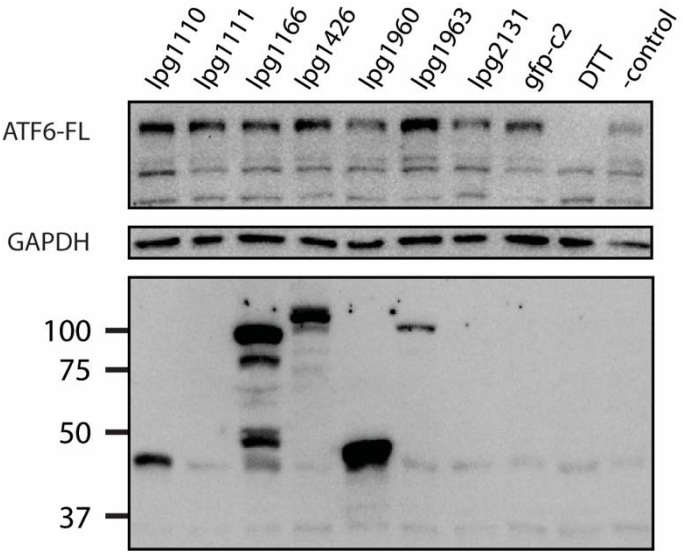

Figure 3.1: Lpg1960 induces ATF6 processing

Immunoblot from HEK293T cells transiently transfected with Myc-tagged effectors. Antibodies against ATF6 (top), GAPDH (middle) and Myc (bottom) are shown. DTT treated cells were treated with 1mM DTT for 1 hr.

Figure 3.2

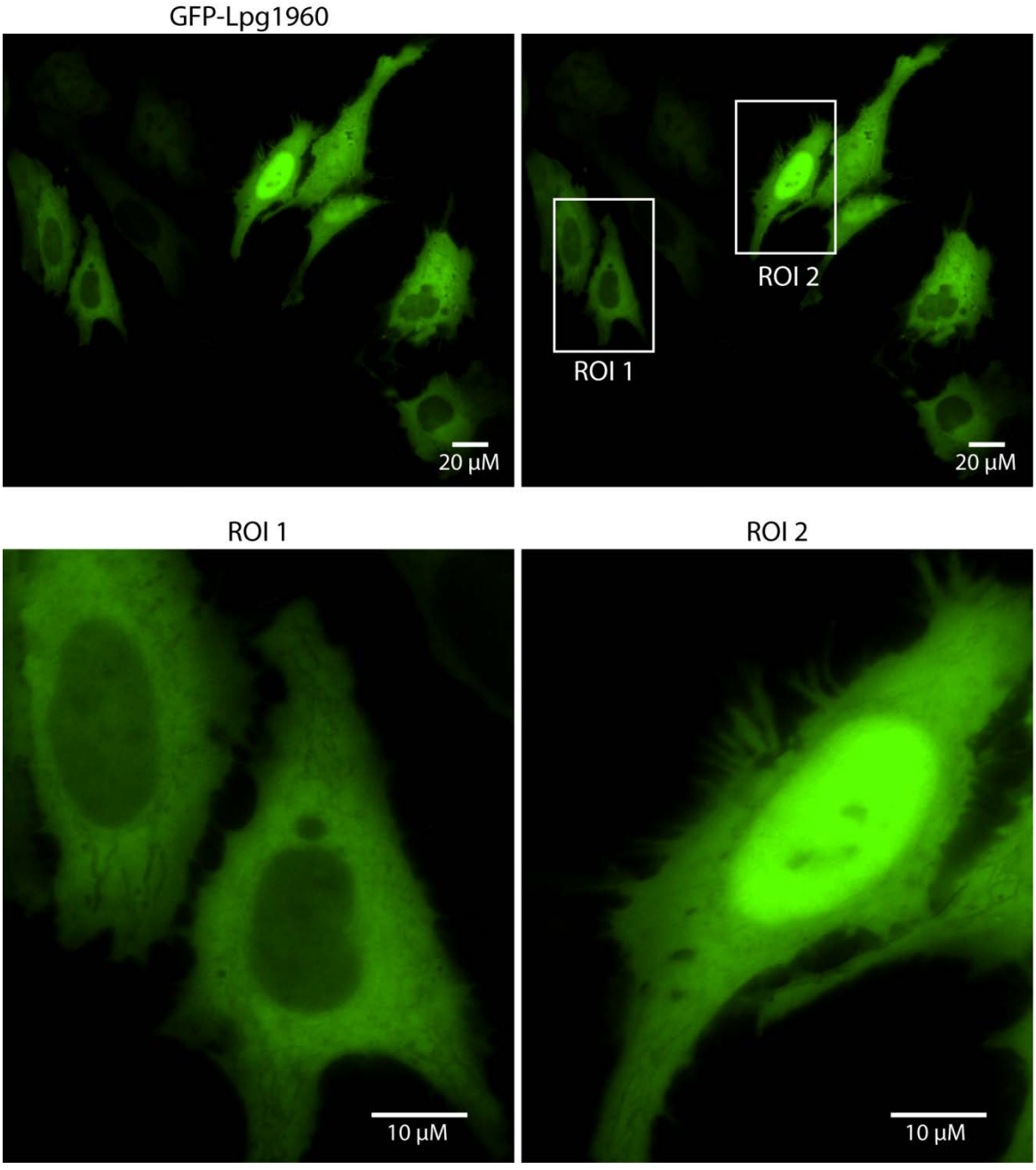

Figure 3.2: GFP-Lpg1960 has a dimorphic localization pattern

Image stills from live cell time lapse widefield microscopy of HeLa cells transiently transfected with GFP tagged Lpg1960 (top), scale bars indicate 20 um distance. Magnified insets from two regions of interest, ROI 1 and ROI 2, scale bars indicate 10 um distance (bottom).

Figure 3.3

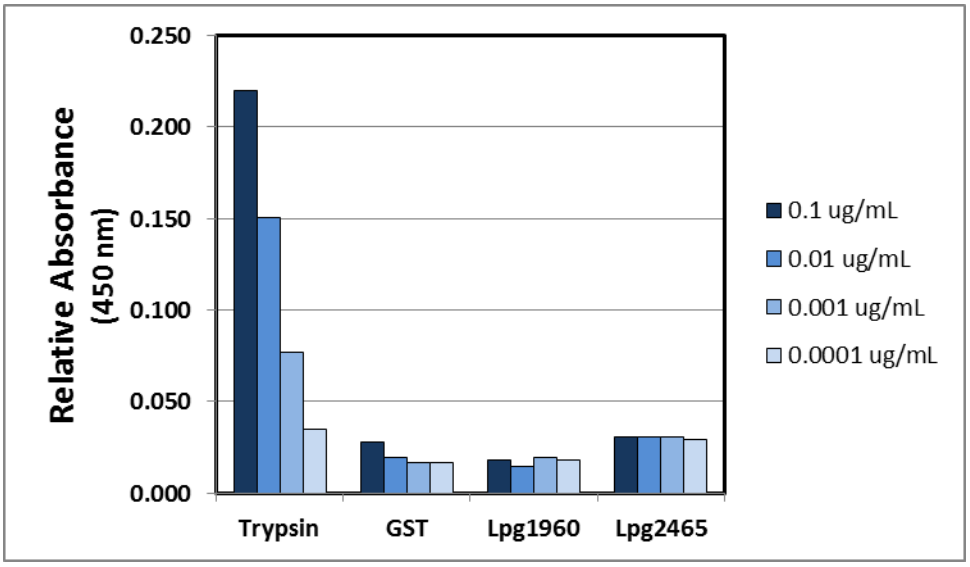

Figure 3.3: Lpg1960 is not catalytically active against casein substrate

10-fold dilution series of TPCK-Trypsin, GST, GST-Lpg1960, and GST-Lpg2465 were assayed using default kit procedure. Absorbance at 450 nm was plotted relative to control well containing substrate only.

Figure 3.4

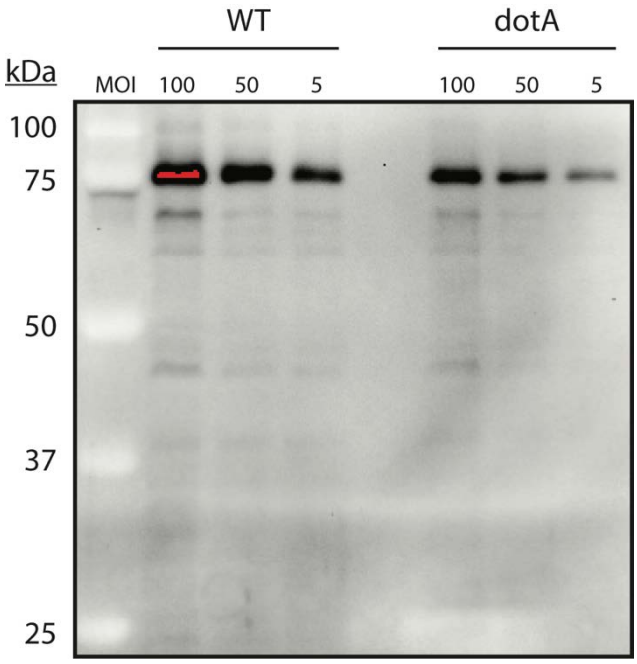

Figure 3.4: ATF6 like protein detected in *L.p.* lysates

Wild type and ΔdotA *L.p*. lysates from exponentially growing liquid cultures were prepared by sonication and immunoblotted using antibodies against human ATF6. Serial dilutions of the indicated MOI are shown.

Figure 3.5

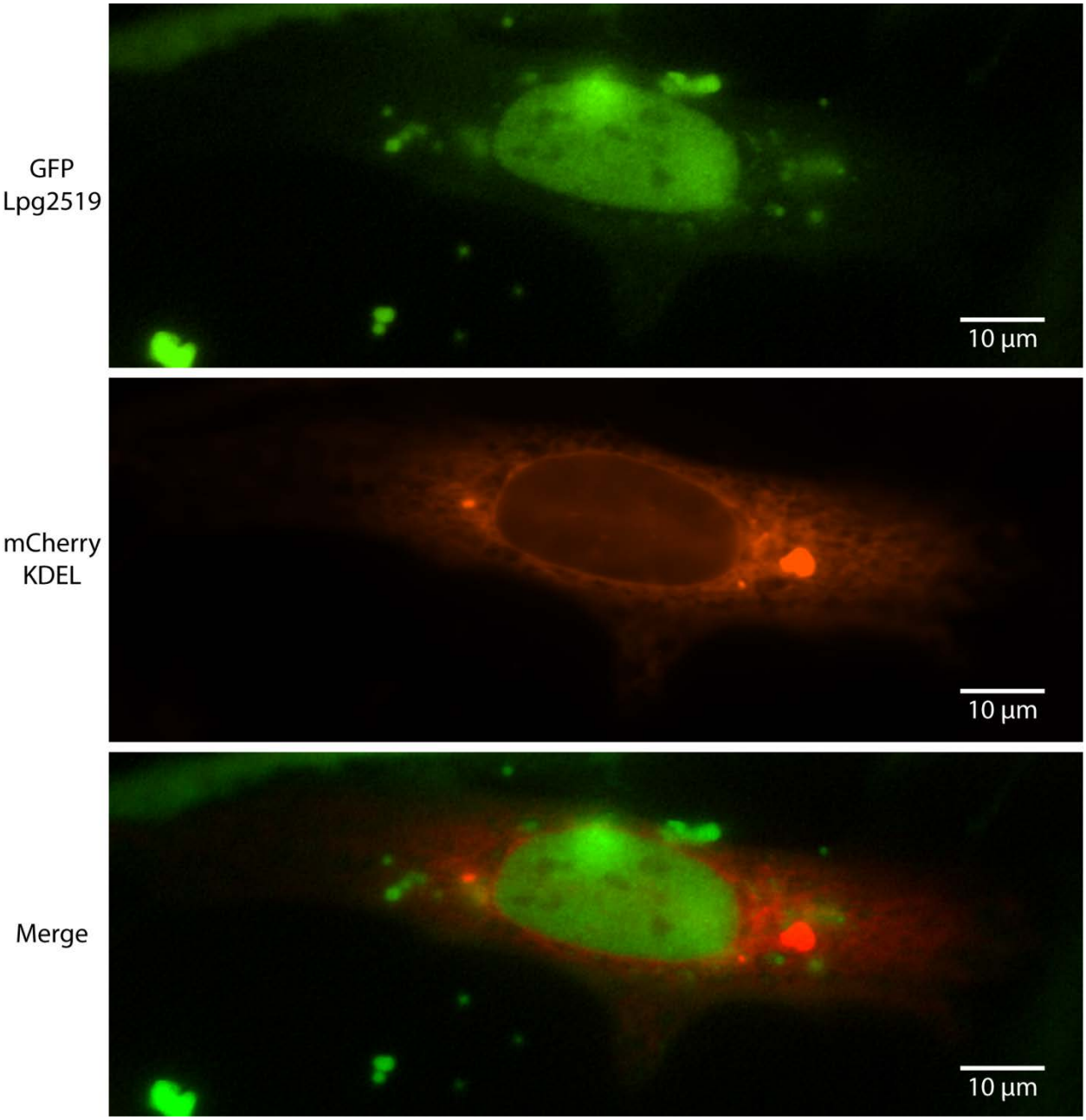

Figure 3.5: Lpg2519 exhibits nuclear localization

Image stills from live cell time lapse widefield microscopy of HeLa cells transiently co-transfected with GFP tagged Lpg2519 (top, green) and mCherry-KDEL (middle, red). Scale bars indicate 10 um distance.

Figure 3.6

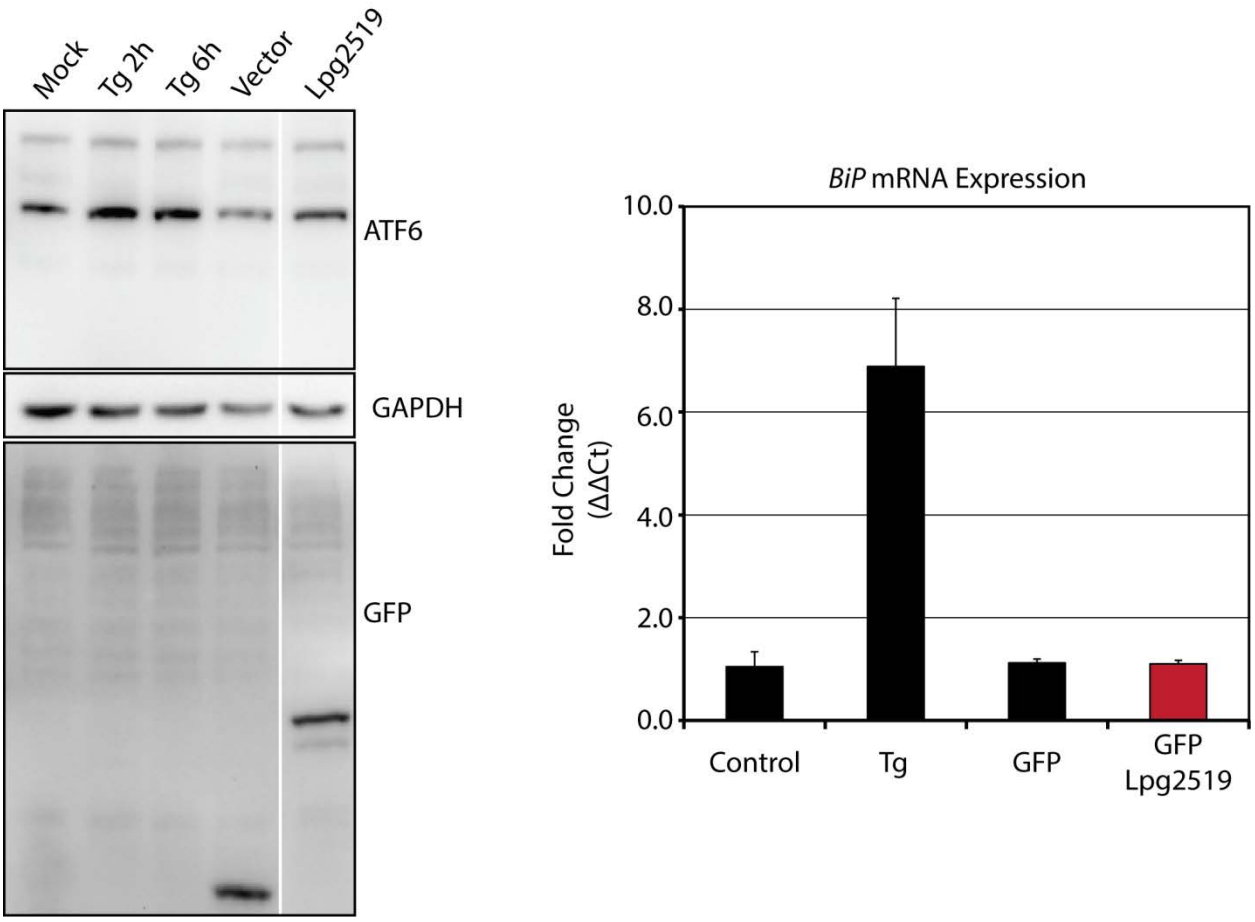

Figure 3.6: Lpg2519 does not activate the ATF6 pathway

Immunoblot from HEK293T cells transiently transfected with the indicated vector, or treated with 200 nM Thapsigargin (Tg) for 2h or 6h. Antibodies against ATF6 (top), GAPDH (middle), and GFP (bottom) were used. *BiP* mRNA levels were analyzed by qPCR from transfected HEK293T cells (right).

References

1) Lifshitz, Z., Burstein, D., Peeri, M., Zusman, T., Schwartz, K., Shuman, H. A., ... & Segal, G. (2013). Computational modeling and experimental validation of the Legionella and Coxiella virulence-related type-IVB secretion signal. Proceedings of the National Academy of Sciences, 110(8), E707-E715.
2) Ke, Y., Wang, Y., Li, W., & Chen, Z. (2015). Type IV secretion system of Brucella spp. and its effectors. Frontiers in cellular and infection microbiology, 5, 72.
3) Belyi, Y., Niggeweg, R., Opitz, B., Vogelsgesang, M., Hippenstiel, S., Wilm, M., & Aktories, K. (2006). Legionella pneumophila glucosyltransferase inhibits host elongation factor 1A. Proceedings of the National Academy of Sciences, 103(45), 16953-16958.
4) Treacy-Abarca, S., & Mukherjee, S. (2015). Legionella suppresses the host unfolded protein response via multiple mechanisms. *Nature communications*, *6*(1), 1-10.
5) Hempstead, A. D., & Isberg, R. R. (2015). Inhibition of host cell translation elongation by Legionella pneumophila blocks the host cell unfolded protein response. *Proceedings of the National Academy of Sciences*, *112*(49), E6790-E6797.
6) Moss, S. M., Taylor, I. R., Ruggero, D., Gestwicki, J. E., Shokat, K. M., & Mukherjee, S. (2019). A Legionella pneumophila kinase phosphorylates the Hsp70 chaperone family to inhibit eukaryotic protein synthesis. Cell host & microbe, 25(3), 454-462.
7) Rawlings, N. D., Barrett, A. J., Thomas, P. D., Huang, X., Bateman, A., & Finn, R. D. (2018). The MEROPS database of proteolytic enzymes, their substrates and inhibitors in 2017 and a comparison with peptidases in the PANTHER database. Nucleic acids research, 46(D1), D624-D632.

8) Schuelein, R., Spencer, H., Dagley, L. F., Li, P. F., Luo, L., Stow, J. L., ... & Sugimoto, C. (2018). Targeting of RNA Polymerase II by a nuclear Legionella pneumophila Dot/Icm effector SnpL. Cellular Microbiology, 20(9), e12852.

9) Li, M., Baumeister, P., Roy, B., Phan, T., Foti, D., Luo, S., & Lee, A. S. (2000). ATF6 as a transcription activator of the endoplasmic reticulum stress element: thapsigargin stress-induced changes and synergistic interactions with NF-Y and YY1. Molecular and cellular biology, 20(14), 5096-5106.

10) Yoshida, H., Matsui, T., Yamamoto, A., Okada, T., & Mori, K. (2001). XBP1 mRNA is induced by ATF6 and spliced by IRE1 in response to ER stress to produce a highly active transcription factor. Cell, 107(7), 881-891.

Chapter 4

Dissertation Conclusions

The use of intracellular pathogens to study biological processes provides many advantages over conventional tools, one being that host-pathogen interactions have evolved over hundreds of millions of years. As such, pathogens are capable of subverting cellular processes that are highly conserved and fundamental to the inner workings of the cell. My study has provided the first example of a bacterial pathogen that exhibits the capacity to activate the ATF6 pathway of the UPR in a manner that bypasses the requirement of conventional pathway components. This observation allows us to consider whether similar activation strategies are conserved within the host cell in the absence of an infection.

The major activation signal for the UPR pathway is the accumulation of unfolded proteins in the ER lumen. It is now becoming apparent that additional input signals can trigger activation of UPR sensors in the absence of unfolded proteins. Changes in the lipid composition within the ER membrane have been shown to trigger activation of the IRE1 and PERK pathways [1]. In either case, removal of the luminal domains of IRE1 and PERK that are responsible for monitoring the unfolded protein status in the ER lumen does not disrupt the sensitivity of these sensors to lipid perturbations. Rather, it was shown that the lipid sensing regions were within the ER-spanning transmembrane domains [2]. Similar to IRE1 and PERK, ATF6 has also been shown to respond to lipotoxic stress within the ER [3]. However, though IRE1 and PERK responded to bulk changes in the lipid composition

within the ER membrane, ATF6 was activated by a specific subset of sphingolipids, dihydrosphingosine and dihydroceramide [3]. Surprisingly, lipid activation of IRE1 and ATF6 induced a transcriptional program that was distinct from the proteotoxic stress-induced transcriptional program [3, 4]. Through our observations, we noted upregulation of both proteotoxic and lipotoxic stress-induced genes during ATF6 activation under *L.p*. infection.

Our results from the ATF6-specific luciferase screen in Chapter 2 implicate multiple *L.p*. effectors in activating the ATF6 pathway. However, the extent by which *L.p*. targets the ATF6 pathway is unclear and whether additional *L.p*. effectors can modulate ATF6 activity remains unknown. The fact that four out of the 17 effectors tested showed a capacity to activate the ATF6 reporter leads me to speculate that additional untested *L.p.* effectors might also impact the ATF6 pathway or UPR more broadly. Additionally, it was not tested whether *L.p*. effectors can act as negative regulators of the ATF6 pathway similar to what is seen with the impact of the Lgt family of effectors on the IRE1 pathway [7]. A thorough survey of all *L.p*. effectors might reveal alternative strategies used to target the UPR pathways.

Our study suggests that activation of ATF6 during *L.p*. infection can occur independently of ATF6 ER-to-Golgi translocation. In this case, the addition of the Ceapin A7 inhibitor blocked pharmacological ATF6 activation, but not ATF6 activation by *L.p.* infection. Yet, we also observed a direct recruitment of ATF6 to the LCV interface at 6 hours post infection when there was no Ceapin A7. The striking correlation in the timing between ATF6-LCV interaction and ATF6 processing would suggest that ATF6 recruitment to the

LCV is a driver of activation. Yet it is not clear whether ATF6 is recruited to the LCV surface in the presence of the Ceapin A7 inhibitor. In this case, a persistent localization of ATF6 to the LCV in the presence of Ceapin A7 inhibitor would also suggest deregulation of ER cargo export, or an alternative trafficking route by which ATF6 exits the ER during *L.p*. infection.

Our data also suggest that ATF6 processing occurs independently of S1P and S2P activity. In fact, mutation of S1P and S2P cleavage sites does not impair ATF6 processing during *L.p.* infection. These data strongly suggest the use of an alternative ATF6 processing sites during infection. Conventionally, ATF6 requires two processing events to liberate the N-terminal ATF6 fragment. The first cleavage is performed by S1P in the ER luminal domain of ATF6. Once the luminal domain is cleaved, ATF6 can then be cleaved by S2P within the transmembrane region. It was shown that without prior cleavage of the luminal domain, the full length ATF6 precursor protein is not a good substrate for S2P cleavage and the presence of a luminal domain in ATF6 prevents S2P activity [5]. Our results suggest ATF6 processing during *L.p.* infection deviates from the conventional pathway. However, it is unknown whether a single *L.p.* effector can catalyze the productive processing of ATF6, individually, or if it is acted upon by additional *L.p*. factors or host proteins.

Beyond our investigations on ATF6, the use of *L.p*. effectors as branch-specific UPR modulators could be a useful tool towards probing the inner workings of the UPR pathways. Many of the well-studied chemical UPR inducers can also cause off target effects within the cell. Thapsigargin acts by depleting calcium (Ca^{2+}) stores within the ER which ultimately alters the activity of Ca^{2+}-dependent chaperones and ER homeostasis. However, the depletion of Ca^{2+} in the ER is accompanied by increased cytosolic Ca^{2+} concentrations.

The by-product could result in changes in activities of proteins and intracellular Ca^{2+} signaling networks such as lipid-acting enzymes that produce bio-reactive molecules [6]. In the end, the broad acting UPR inducers might cause cellular changes that could obfuscate the true functions of the UPR sensors. If *L.p*. effectors are found that can act directly on the UPR sensors to activate or inhibit their function, many fundamental questions can be probed to understand the contributions of each sensor towards the overall homeostatic response.

Altogether, further experimentation will help elucidate molecular mechanisms underlying the unconventional activation of ATF6 during *L.p*. infection. Understanding how *L.p*. activates the ATF6 pathway would not only provide additional examples of how pathogens subvert UPR function, but could also lead to the discovery of novel host strategies that act in a similar fashion. Expanding upon this research by screening more broadly for *L.p*. effectors that can target each branch of the UPR might lead to the discovery of novel UPR regulators. Furthermore, the use of *L.p.* effectors as an alternative to chemical agents to modulate UPR activity might permit more sensitive investigations into the functions of the individual sensors or the UPR in its entirety.

References

1) Volmer, R., van der Ploeg, K., & Ron, D. (2013). Membrane lipid saturation activates endoplasmic reticulum unfolded protein response transducers through their transmembrane domains. Proceedings of the National Academy of Sciences, 110(12), 4628-4633.
2) Halbleib, K., Pesek, K., Covino, R., Hofbauer, H. F., Wunnicke, D., Hänelt, I., ... & Ernst, R. (2017). Activation of the unfolded protein response by lipid bilayer stress. Molecular cell, 67(4), 673-684.
3) Tam, A. B., Roberts, L. S., Chandra, V., Rivera, I. G., Nomura, D. K., Forbes, D. J., & Niwa, M. (2018). The UPR activator ATF6 responds to proteotoxic and lipotoxic stress by distinct mechanisms. Developmental cell, 46(3), 327-343.
4) Ho, N., Yap, W. S., Xu, J., Wu, H., Koh, J. H., Goh, W. W. B., ... & Thibault, G. (2020). Stress sensor Ire1 deploys a divergent transcriptional program in response to lipid bilayer stress. Journal of Cell Biology, 219(7).
5) Shen, J., & Prywes, R. (2004). Dependence of site-2 protease cleavage of ATF6 on prior site-1 protease digestion is determined by the size of the luminal domain of ATF6. Journal of Biological Chemistry, 279(41), 43046-43051.
6) Joseph, S. K., & Hajnóczky, G. (2007). IP 3 receptors in cell survival and apoptosis: Ca 2+ release and beyond. Apoptosis, 12(5), 951-968.
7) Treacy-Abarca, S., & Mukherjee, S. (2015). Legionella suppresses the host unfolded protein response via multiple mechanisms. Nature communications, 6(1), 1-10.

Publishing Agreement

It is the policy of the University to encourage open access and broad distribution of all theses, dissertations, and manuscripts. The Graduate Division will facilitate the distribution of UCSF theses, dissertations, and manuscripts to the UCSF Library for open access and distribution. UCSF will make such theses, dissertations, and manuscripts accessible to the public and will take reasonable steps to preserve these works in perpetuity.

I hereby grant the non-exclusive, perpetual right to The Regents of the University of California to reproduce, publicly display, distribute, preserve, and publish copies of my thesis, dissertation, or manuscript in any form or media, now existing or later derived, including access online for teaching, research, and public service purposes.

DocuSigned by:
Nnejiuwa Ibe
38CCC1DBF891433...
Author Signature

8/28/2020
Date